

Palestine Polytechnic University



College of Engineering

Civil & Architectural Engineering Department

Surveying and Geomatics Engineering

Graduation Project

The use of mobile phone camera in close range photogrammetry

Ahmad Atatrah

Ahmad Mujahed

Anan Kittani

Supervisor:

DR. Ghadi Zakarneh

Hebron-West Bank

Palestine

May-2014

الإهداء

نهدي هذا المشروع لكل معلم وهاد للبشرية ، لكل من غرس بذور العلم والمعرفة .
لكل من رعى برعما وأصل خلقا وأكفل يتيما ورحم مسكينا ولكل من عرف معنى الإنسانية
بقلب وروح الإنسان .
نهدي هذا العمل إلى من كافح في دنياه فتحمل ويلات الزمن وتجرع علقم السنين فاعتصر
الصخر وأخفى آلامه عنا كي لا نشعر بقسوة الحياة .
إلى الماس الذي لا ينكسر ، ونبع العطاء الذي زرع الخلق والقيم المثلى وعلمنا طرق
الارتقاء .
إلى من تعجز الكلمات عن وصفه وتسكن أمواج البحر لسماع صوته ، إلى من كنت له
الأمل الذي راوده في حياته فلم أن يراني في مثل هذا اليوم ... أبي الحبيب .
نهدي هذا العمل إلى من كانت جنة مليئة بورد الحب ، إلى الإنسانة الغالية الصابرة ،
والقمر الذي ينير دربي وحياتي .
إلى البلسم الذي يشفي جراحي والياسمين الذي يعطر طريقي ، إلى من سهرت حتى كبرت
ونشأت .
إلى أغلى جوهرة في العالم ، تلك الشجرة الباسقة في وجه أعاصير الحياة ترنو بأغصانها
إلى السماء متضرعة دعاء لي ... أمي الحبيبة .
نهدي هذا العمل إلى القلوب التي ترتقب عودتي بصبر ، وتفرح الروح لذكراهم وتسر
العيون للقياهم .
إلى شقائق النعمان الذين احتضنوني وزرعوا الورد في طريقي ... إخوتي وأخواتي .
نهدي هذا العمل إلى كل من يحمل مودة في قلبي ، رفاق الدرب بناء المستقبل على طريق
الشهداء .
حملة رسالة الأسرى والجرحى والمبعدة واللاجئين ، من رفعوا رايات العلم والتعليم
واخمدوا نار الجهل والتجهيل ... زملائنا وزميلاتنا .
نهدي هذا العمل إلى الروح التي اختارها الله لتكون بريق شهادة في طريق العلم ، إلى
الجسد الذي أبكنا فراقه حبا وحزنا وخجلا .
إلى أهله وذويه وروحه الطاهرة ... المرحوم الصديق المهندس أسيد طوافشة .
نهدي هذا العمل لكل زاوية في جامعتنا الحبيبة ، ولكل قلم وورقة وخط ، ولمن ساهم
بايصالنا لهذه الرسالة السامية .
نهدي هذا العمل لكل من بذل دقيقة تعب وتوجيه من أساتذتنا الأفاضل وطاقم الجامعة
الأكاديمي والإداري .
ولكل من طاب ذكره ، وانشرح صدره برسالة التعلم ، وكان مصدر دعم لنا ولطالبة
فلسطين ، ولعبق الأرض الطاهرة - فلسطين - نهدي هذا العمل

Acknowledgment

Our special thanks to our supervisor Dr.Ghadi Zakarneh Also we want to thank the Palestinian Department of survey.

Finally, we extended our thank to members in the Civil Engineering Dept. Especially the part of Surveying Engineering, which help us in designing our project.

Abstract

The use of mobile phone camera in close range photogrammetry

Group names

Ahmad Atatrah

Ahmad Mujahed

Anan Kittani

Supervisor

Dr.Ghadi Zakarneh

Abstract:

The project aims to use a simple technology owned by anyone in close range photogrammetry, such as use of different mobile cameras to make a 3D modeling of close objects by using a lot of software. These camera are now a days available with high resolution in different levels. So we are going to study the use of these cheap tools in the fields of close range photogrammetry.

The project requires three stages. First we are going to test the use of the photos for 3D modeling of close range objects. Then, we are going to compare results. And finally, introduce camera calibration for each mobile camera.

ملخص المشروع

استخدام كاميرا الهاتف الجوال في التصوير الارضي

أسماء الطلاب

أحمد عطا طره

أحمد مجاهد

عنان كنانه

المُشرف

د. غادي زكارنة

الملخص:

يهدف المشروع لاستخدام التكنولوجيا البسيطة المتوفرة مع الجميع في التصوير الارضي. مثل استخدام أنواع مختلفة من كاميرات الهاتف الجوال لعمل مجسم ثلاثي الابعاد من خلال استخدام العديد من البرامج. هذه الكاميرات في هذه الأيام متاحة بدقة تصوير عالية بمستويات مختلفة. لذلك سوف نقوم بدراسة استخدام أدوات رخيصة الثمن في حقول التصوير الأرضي.

ويتم عمل هذا المشروع على عدة مراحل ، أولها اختبار الصور لعمل مجسم ثلاثي الابعاد. وبعد ذلك يتم مقارنة الصور مع بعضها البعض. واخيرا نقوم بعمل المعايرة لكل كاميرا استخدمت في التصوير .

Table of Contents

اهداء	II
ACKNOWLEDGMENTS	III
ABSTRACT	IV
ملخص	V
TABLE OF CONTENTS	VI
TABLE OF FIGURE	IX
TABLE OF TABELS	XII
CHAPTER ONE: INTRODUCTION	1
1.1 INTRODUCTION	1
1.2 OBJECTIVE	2
1.3 TIME TABLE	2
1.4 METHODOLOGY	3
1.5 PROJECT SCOPE	3
CHAPTER TWO: INTRODUCTION TO PHOTOGRAMMETRY	5
2.1 DEFINITION OF PHOTOGRAMMETRY	6
2.2 HISTORY OF PHOTOGRAMMETRY	7
2.3 TYPES OF PHOTOGRAPHS	8
2.4 CLOSE RANGE CAMERAS	8
2.5 AERIAL PHOTOGRAPHY	10
2.6 FIELDS OF PHOTOGRAMMETRY	12
CHAPTER THREE: CLOSE RANGE PHOTOGRAMMETRY	17
3.1 INTRODUCTION	18
3.2 TERRESTRIAL CAMERAS	18

3.3	HORIZONTAL AND OBLIQUE TERRESTRIAL PHOTO	20
3.4	CAMERA INCLINATION	21
3.5	MEASURING HORIZONTAL AND VERTICAL ANGLES	24
3.6	CAMERA AXIS AND EXPOSURE STATION POSITION	25
3.7	CALCULATION OF POINTS POSITION	26
3.8	ANALYTICAL SOLUTION FOR CLOSE RANGE PHOTOGRAMMETRY	28
CHAPTER FOURE: APPLICATION OF CLOSE RANGE PHOTOGRAMMETRY		30
4.1	INTRODUCTION	31
4.2	ACCIDENT RECONSTRUCTION	31
4.3	CRIME SCENE	32
4.4	STRUCTURAL ANALYSIS	33
4.5	VOLUME COMPUTING	35
4.6	FACIAL RECOGNITION	37
4.7	DOCUMENTATION OF CULTURAL (FATIH MOSQUE)	40
CHAPTER FIVE: CAMERA CALIBRATION		41
5.1	INTRODUCTION	42
5.2	ELEMENTS OF INTERIOR ORIENTATION	43
5.2.1	CALIBRATED FOCAL LENGTH	43
5.2.2	SYMMETRIC RADIAL LENS DISTORTION	43
5.2.3	DECENTERING LENS DISTORTION	43
5.2.4	PRINCIPAL POINT LOCATION	45
5.2.5	FIDUCIAL MARK COORDINATES	45
5.3	LABORATORY METHODS OF CAMERA CALIBRATION	45
5.4	STELLAR METHODS	46
5.5	FIELD METHODS	47
5.6	ANALYTICAL SELF CALIBRATION	47
5.7	AUTOMATIC CAMERA CALIBRATION	49
5.8	COMPUTATION OF SELF CALIBRATION	50
5.9	TEST FIELD	51
5.10	ZOOM DEPENDENT CAMERA CALIBRATION	52
5.11	Z-D CALIBRATION MODEL	52

CHAPTER SIX: RESULTS AND ANALYSIS	54
6.1 INTRODUCTION	55
6.2 USED SOFTWARE	55
6.2.1 INSIGHT3D	55
6.2.2 AGISOFT STEREOSCAN	56
6.2.3 123D CATCH	57
6.2.4 MESH LAB	58
6.2.5 AGISOFT LENZ	59
6.3 USED HARDWARE	61
6.3.1 NOKIA X3	61
6.3.2 I PHONE 4G	63
6.3.3 I PHONE 5S	64
6.4 CAMERA CALIBRATION	65
6.5 RESULTS	67
6.5.1 MODEL #1	67
6.5.1.1 NOKIA X3	68
6.5.1.2 I PHONE 4G	70
6.5.1.3 I PHONE 5S	71
6.5.2 MODEL #2	73
6.5.2.1 NOKIA X3	73
6.5.2.2 I PHONE 4G	75
6.5.2.3 I PHONE 5S	77
6.5.3 MODEL #3	73
6.5.3.1 NOKIA X3	78
6.5.3.2 I PHONE 4G	80
6.5.3.3 I PHONE 5S	81
6.5.4 MODEL #4	82
6.5.4.1 NOKIA X3	83
6.5.4.2 I PHONE 4G	85
6.5.4.3 I PHONE 5S	86
6.6 PRACTICAL EXAMPELS	87
6.1.1 OLD BUILDING	87
6.1.1 IBRAHIMI MOSQUE	89
6.1.1 CEMETERY	90

CHAPTER SEVEN: CONCLUSION AND RECOMMENDATION	91
7.1 CONCLUSION	92
7.2 RECOMMENDATION	93
REFERENCES	95

Table of Figures

CHAPTER TWO: INTRODUCTION TO PHOTOGRAMMETRY

FIGURE (2-1): TERRESTRIAL PHOTOGRAPH	9
FIGURE (2-2): PHOTOTHEODOLITE	9
FIGURE (2-3): BALLISTIC CAMERA	10
FIGURE (2-4): AERIAL CAMERA, WITH ELECTRONIC AND AIRCRAFT MOUNTINGS	11
FIGURE (2-5): CAMERA ORIENTATION FOR VARIOUS TYPES OF AERIAL PHOTOGRAPHS	12
FIGURE (2-6): DIGITAL ELEVATION MODELS	13
FIGURE (2-7): ORTHO MAP	13
FIGURE (2-8): BASE MAP	14
FIGURE (2-9): 3D GLASS FOR STEREOSCOPIC VIEWING	15
FIGURE (2-10): X-RAY PHOTO	16

CHAPTER THREE: CLOSE RANGE PHOTOGRAMMETRY

FIGURE (3-1): PHOTOTHEODOLITE	19
FIGURE (3-2): STEREOMETRIC CAMERA SYSTEM	20
FIGURE (3-3): CAMERA AXIS	21
FIGURE (3-4): HORIZONTAL AND VERTICAL ANGELS FROM MEASUREMENTS ON AN OBLIQUE	21
FIGURE (3-5): LOCATION OF HORIZON AND NADIR ON AN OBLIQUE PHOTOGRAPH	22
FIGURE (3-6): OBLIQUE PHOTO COORDINATE AXIS SYSTEM	23
FIGURE (3-7): HORIZONTAL AND VERTICAL ANGELS FROM MEASUREMENTS ON AN OBLIQUE TERRESTRIAL PHOTO	24
FIGURE (3-8): DETERMINING ELEVATION OF CAMERA STATION OF TERRESTRIAL PHOTO BY USING ONE VERTICAL CONTROL POINT	25
FIGURE (3-9): GRAPHICAL THREE POINT RESECTION TO LOCATE EXPOSURE STATION AND DIRECTION OF OPTICAL AXIS	25

FIGURE (3-10): LOCATING POINTS BY INTERSECTION FROM TWO OBLIQUE TERRESTRIAL PHOTOS	27
FIGURE (3-11): PLAN VIEW OF INTERSECTION FROM TWO OBLIQUE TERRESTRIAL PHOTOS	27
FIGURE (3-12):	29

CHAPTER FOUR: APPLICATION OF CLOSE RANGE PHOTOGRAMMETRY

Figure (4-1): Analyze the dynamics of the collision event	31
Figure (4-2): Example of images of crime scene	33
Figure (4-3): Close-Range Photogrammetric Measurement for Structural Analysis	35
Figure (4-4): Study area	37
Figure (4-5): Post Excavation	37
Figure (4-6): Image capturing based on three different positions	39
Figure (4-7): Interest points of the face	39

CHAPTER FIVE: CAMERA CALIBRATION

FIGURE (5-1): TYPICAL SYMMETRIC RADIAL LENS	44
FIGURE (5-2): TYPICAL DECENTERING DISTORTION	44
Figure (5-3): combined symmetric radial and decentering distortion	45
Figure (5-4): 13 collimators for camera calibration	46
Figure (5-5): The test field	51
Figure (5-6): The distribution of exposure stations	51

CHAPTER SIX: RESULTS AND ANALYSIS

FIGURE (6-1): THE MAIN INTERFACE OF INSIGHT 3D	56
FIGURE (6-2): 3D MODEL USING SAMSUNG GALAXY S4 IN AGISOFT STEREOSCAN	57
FIGURE (6-3): THE MAIN INTERFACE OF 123D CATCH	58
FIGURE (6-4): THE MAIN INTERFACE OF MESH LAB	59
FIGURE (6-5): CHESSBOARD	60
FIGURE (6-6): THE MAIN INTERFACE OF AGISOFT LENZ	61
FIGURE (6-7): NOKIA X3	62
FIGURE (6-8): I PHONE 4G	63
FIGURE (6-9): I PHONE 5S	64
FIGURE (6-10): CAMERA CALIBRATION FOR NOKIA X3 MOBILE PHONE	65
FIGURE (6-11): CAMERA CALIBRATION FOR I PHONE 4G MOBILE PHONE	66

FIGURE (6-12): CAMERA CALIBRATION FOR I PHONE 5S MOBILE PHONE	66
FIGURE (6-13): CAMERA CALIBRATION FOR SAMSUNG GALAXY S4 MOBILE PHONE	67
FIGURE (6-14): MODEL #1	68
FIGURE (6-15): MODEL #1 BY NOKIA X3 IN MESHLAB	69
FIGURE (6-16): MODEL #1 BY I PHONE 4G IN MESHLAB	70
FIGURE (6-17): MODEL #1 BY I PHONE 5S IN MESHLAB	72
FIGURE (6-18): MODEL #2	73
FIGURE (6-19): MODEL #2 BY NOKIA X3 IN MESHLAB	74
FIGURE (6-20): MODEL #2 BY I PHONE 4G IN MESHLAB	75
FIGURE (6-21): MODEL #2 BY I PHONE 5S IN MESHLAB	76
FIGURE (6-22): MODEL #3	78
FIGURE (6-23): MODEL #3 BY NOKIA X3 IN MESHLAB	79
FIGURE (6-24): MODEL #3 BY I PHONE 4G IN MESHLAB	80
FIGURE (6-25): MODEL #3 BY I PHONE 5S IN MESHLAB	81
FIGURE (6-26): MODEL #4	83
FIGURE (6-27): MODEL #4 BY NOKIA X3 IN MESHLAB	84
FIGURE (6-28): MODEL #4 BY I PHONE 4G IN MESHLAB	85
FIGURE (6-29): MODEL #4 BY I PHONE 5S IN MESHLAB	86
FIGURE (6-30): OLD BUILDING	88
FIGURE (6-31): OLD BUILDING IN MESHLAB	88
FIGURE (6-32): ALQHAR ALSHAREEF	89
FIGURE (6-33): ALQHAR ALSHAREEF IN MESHLAB	89
FIGURE (6-34): MENBER SALAH ALDEEN	90
FIGURE (6-35): MENBER SALAH ALDEEN IN MESHLAB	90
FIGURE (6-36): CEMETERY AS PHOTO	91
FIGURE (6-37): CEMETERY AS 3D MODEL	91

Table of tables

TABLE (1-1): TIME SCHEDULE FOR FIRST SEMESTER	3
TABLE (6-1): NOKIA X3 PROPERTIES	62
TABLE (6-2): I PHONE 4G PROPERTIES	63
TABLE (6-3): I PHONE 5S PROPERTIES	64

TABLE (6-4): MODEL #1 BY NOKIA X3 RESULTS	69
TABLE (6-5): MODEL #1 BY I PHONE 4G RESULTS	71
TABLE (6-6): MODEL #1 BY I PHONE 5S RESULTS	72
TABLE (6-7): MODEL #2 BY NOKIA X3 RESULTS	74
TABLE (6-8): MODEL #2 BY I PHONE 4G RESULTS	75
TABLE (6-9): MODEL #2 BY I PHONE 5S RESULTS	77
TABLE (6-10): MODEL #3 BY NOKIA X3 RESULTS	79
TABLE (6-11): MODEL #3 BY I PHONE 4G RESULTS	80
TABLE (6-12): MODEL #3 BY I PHONE 5S RESULTS	82
TABLE (6-13): MODEL #4 BY NOKIA X3 RESULTS	84
TABLE (6-14): MODEL #4 BY I PHONE 4G RESULTS	85
TABLE (6-15): MODEL #4 BY I PHONE 5S RESULTS	87

CHAPTER ONE

INTRODUCTION

1.1 Background

1.2 Objective

1.3 Time Schedule

1.4 Methodology

1.5 Project Scope

1.1 Background

Terrestrial photogrammetry is an important branch of the photogrammetric science. It deals with photographs taken with cameras located on or near the surface of the earth. The term close range photogrammetry is generally used for terrestrial photographs having object distances up to about 300 m. Terrestrial photography can applied in two ways:

- Static: photos stationary objects. Stereopairs can be obtained by using a single camera and making exposures at both ends of a baseline or two different cameras.
- Dynamic: photos of moving objects. Two cameras located at the ends of a baseline must make simultaneous exposures.

1.2 Objective

This project aims to use a simple technology owned by anyone in close range photogrammetry. For example, the use of different mobile phone cameras to make 3D models of close objects by using different software. Mobile phone nowadays is available with high resolution cameras in different levels of mega pixels. So we are going to study the use of these cheap tools in the fields of close range photogrammetry by taking the advantage of the cheap or freely available modeling software.

1.3 Time Table:

The time schedule shows the stages for achieving our work and the process of project growth. The time schedule includes Project determination, literature review, collecting data, designing the entire system. Table (1-1) shows the first semester project growth. All tasks are referred to the theoretical background and the whole system analysis.

Table (1 - 1) Time Schedule for first semester

Weeks Tasks	1	2	3	4	5	6	7	8	9	10	11	12	13	14	15	16
Project idea	→															
Project analysis and plane			→													
Training on using 3D Programs					→											
Selection of Models								→								
Chose the best model										→						
Presentation																★
Weeks Tasks	17	18	19	20	21	22	23	24	25	26	27	28	29	30	31	32
Observation of points	→															
Scaling Models										→						
Data Analysis														→		
Presentation																★

1.4 Methodology

Method of working on this project is to be achieved by taking several pictures using mobile phone cameras. Afterwards we are going to Install the taken pictures to create 3D models using different software that are available in the university (PPU) or online for free. Finally the mobile camera will be calibrated to make a model more precise.

1.5 Project Scope

This project consists of five chapters as follows:

- Chapter One: An introduction of the project and its description.
- Chapter Two: Introduction to photogrammetry that introduces the history of the photogrammetry

- Chapter Three: Introduces close range photogrammetry and its principles.
- Chapter four: Discusses some applications of close range photogrammetry
- Chapter five: Introduces different methods for photogrammetry camera calibration.

CHAPTER TWO

INTRODUCTION TO PHOTOGRAMMETRY

- 2.1 **Definition of Photogrammetry**
- 2.2 **History of Photographs**
- 2.3 **Types of Photographs**
- 2.4 **Close Range Cameras**
- 2.5 **Aerial Photography**
- 2.6 **Fields of Photogrammetry**

2.1 Definition Of Photogrammetry

Photogrammetry is defined as the art, science, and technology of obtaining reliable information about physical objects and the environment through processes of recording, measuring, and interpreting photographic images and patterns of recorded radiant electromagnetic energy and other phenomena, as defined by photogrammetry is applied by science analyzing photographs. By technological development, photogrammetry has expanded to include the following fields:

1. Digital imagery.
2. Radiated acoustical energy patterns.
3. Laser ranging measurements.
4. Magnetic phenomena.

Photographs are still the principal source of information. In this text photographic and digital photogrammetry are emphasized, but other sources of information are also discussed. Photogrammetry includes two specific areas:

1. Metric photogrammetry.
2. Interpretative photogrammetry.

Metric photogrammetry consists of making precise measurements from photos and other information sources to determine, in general, the relative locations of points. This enables finding distances, angles, areas, volumes, elevations, and sizes and shapes of objects. The most common applications of metric photogrammetry are the preparation of planimetric and topographic maps from photographs, and the production of digital orthophotos from scanned photography. The photographs are most often aerial, taken from an airborne vehicle, but close range photos ,taken from earth-based cameras and satellite imagery are also used.

Interpretative photogrammetry deals principally in recognizing and identifying objects and judging their significance through careful and systematic analysis. It includes branches of photographic interpretation and remote sensing. Photographic interpretation

includes the study of photographic images, while remote sensing includes not only the analysis of photography but also the use of data gathered from a wide variety of sensing instruments, including multispectral cameras, infrared sensors, thermal scanners, and side-looking airborne radar.

2.2 History Of Photogrammetry

In the early 18th century Dr. Brook Taylor published his treatise on linear perspective, and soon afterward, J. H. Lambert suggested that the principles of perspective could be used in preparing maps.

The actual practice of photogrammetry could not occur, of course, until a practical photographic process was developed. This occurred in 1839, when Louis Daguerre of Paris announced his direct photographic process. In his process the exposure was made on metal plates that had been light-sensitized with a coating of silver iodide. This is essentially the photographic process in use today.

The first actual experiments in using photogrammetry for topographic mapping occurred in 1849 under the direction of Colonel Aime Laussedat of the French Army Corps of Engineers. In Colonel Laussedat's experiments kites and balloons were used for taking aerial photographs. Due to difficulties encountered in obtaining aerial photographs, he curtailed this area of research and concentrated his efforts on mapping with terrestrial photographs. In 1859 Colonel Laussedat presented an accounting of his successes in mapping using photographs. His pioneering work and dedication to this subject earned him the title "father of photogrammetry."

Topographic mapping using photogrammetry was introduced to North America in 1886 by Captain Eduard Deville, the Surveyor General of Canada. He found Laussedat's principles extremely convenient for mapping the rugged mountains of western Canada. The U.S. Coast and Geodetic Survey, now the National Geodetic Survey, adopted

photogrammetry in 1894 for mapping along the border between Canada and the Alaska Territory.

2.3 Types Of Photographs

Two fundamental classifications of photography used in the science of photogrammetry are close range and aerial. Close range photographs are taken with ground based cameras, the position and orientation of which are often measured directly at the time of exposure.

2.4 Close Range Cameras

A great variety of cameras are used for taking terrestrial photographs, and these may include:

1. Hobby cameras, which are handheld.
2. Phototheodolite: is a combination camera and theodolite mounted on a tripod used for taking terrestrial photographs. The theodolite, a surveying instrument which is used to measure angles, facilitates aligning the camera in a desired or known azimuth and measuring its position and elevation. Figure (2-1) shows a terrestrial photograph taken with a camera of the type phototheodolite shown in Fig. (2-2).
3. ballistic camera : These large cameras were mounted at selected ground stations and used to obtain photographs of orbiting artificial satellites against a star background. The photographs were analyzed to calculate satellite trajectories; the size, shape, and gravity of the earth; and the precise positions of the camera stations. This procedure utilized precisely known camera constants, together with the known positions of the background stars at the instants of exposure. Ballistic cameras played an essential role in establishing a worldwide network of control points and in accurately determining the relative positions of the continents,

remote ocean islands, etc. Use of ballistic cameras for this purpose has been made obsolete by the Global Positioning System (GPS), a network of transmitting satellites and ground based receivers which enables extremely accurate positions to be determined anywhere on or near the earth as shown in figure (2-3).



Figure (2 - 1) terrestrial photograph . [9]



Figure (2 - 2) phototheodolite . [10]



Figure (2 - 3) Ballistic camera . [11]

2.5 Aerial Photography

commonly classified as either vertical or oblique. Vertical photos are taken with the camera axis directed as nearly vertically as possible. If the camera axis were perfectly vertical when an exposure was made, the photographic plane would be parallel to the datum plane and the resulting photograph would be termed truly vertical. In practice, the camera axis is rarely held perfectly vertical due to unavoidable aircraft tilts. When the camera axis is unintentionally tilted slightly from vertical, the resulting photograph is called a tilted photograph. These unintentional tilts are usually less than 1° and seldom more than 3° . For many practical applications, simplified procedures suitable for analyzing truly vertical photos may also be used for tilted photos without serious consequence. Precise photogrammetric instruments and procedures have been developed, however, that make it possible to rigorously account for tilt with no loss of accuracy. Figure (2-4) shows an aerial camera with its electric control mechanism.

Oblique aerial photographs are exposed with the camera axis intentionally tilted away from vertical. A high oblique photograph includes the horizon, a low oblique does not. Figure (2-5) illustrates the orientation' of the camera for vertical, low oblique, and high oblique photography and also shows how a square grid of ground lines would appear in each of these types' of photographs.



Figure (2 - 4) Aerial camera, with electronic and aircraft mountings. [12]

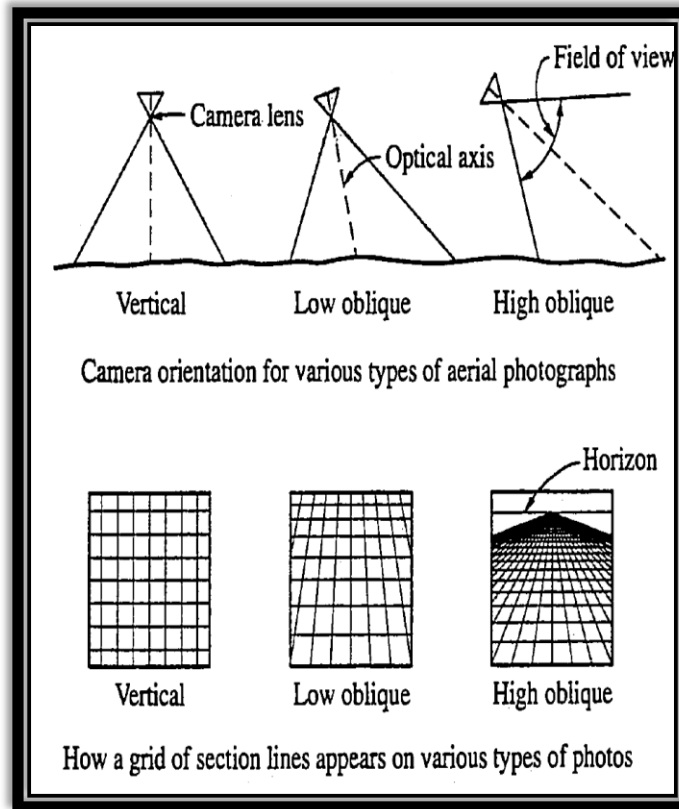


Figure (2 - 5) Camera orientation for various types of aerial photographs . [1]

2.6 Fields Of Photogrammetry

Earliest applications of photogrammetry were in topographic mapping, and today that use is still the most common of photogrammetric activities.

Two newer photogrammetric products, orthophotos, and digital elevation models. (DEMs), are now often used in combination to replace traditional topographic maps as shown in figure (2-6). An orthophoto, is an aerial photograph that has been modified so that its scale is uniform throughout, as shown in figure (2-7). Thus orthophotos are equivalent to planimetric maps, but unlike planimetric maps which show features by means of lines and symbols, orthophotos show the actual images of features. For this reason they are more easily interpreted than planimetric maps, and hence are preferred by many users.



Figure (2 - 6) Digital elevation models . [12]



Figure (2 - 7) Ortho map

Photogrammetry has become an exceptionally valuable tool in land surveying. To mention just a few uses in the field, aerial photos can be used as rough base maps for

relocating existing property boundaries as shown in figure (2-8). If the point of beginning or any corners can be located with respect to ground features that can be identified on the photo, the entire parcel can be plotted on the photo from the property description. All corners can then be located on the photo in relation to identifiable ground features which, when located in the field, greatly assist in finding the actual property corners.

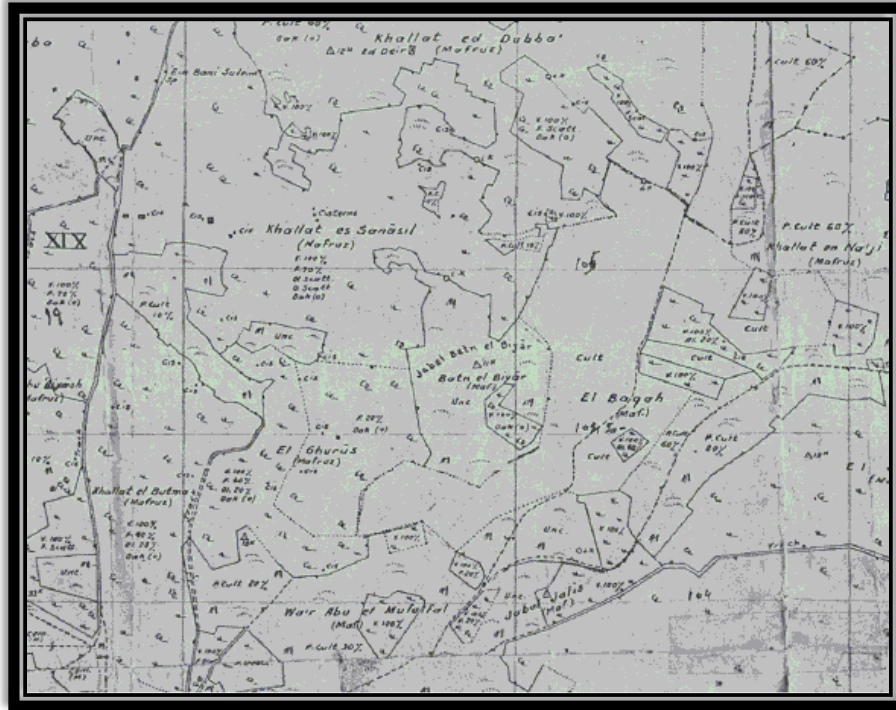


Figure (2 - 8) Base map . [15]

Aerial photos can also be used in planning ground surveys. Through stereoscopic viewing with 3D glasses as shown in figure (2-9), the area can be studied in three dimensions. Access routes to remote areas can be identified and surveying lines of least resistance through difficult terrain or forests can be found. The photogrammetrist can prepare a map of an area without actually setting foot on the ground an advantage which circumvents problems of gaining access to private land for ground surveys.



Figure (2 - 9) 3D glass for stereoscopic viewing . [13]

Many areas outside of engineering have also benefitted from photogrammetry. Nonengineering applications include the preparation of tax maps, soil maps, forest maps, geologic maps, and maps for city and regional planning and zoning. Photogrammetry is used in the fields of astronomy, architecture, archaeology, geomorphology, oceanography, hydrology and water resources, conservation, ecology, and mineralogy.

Photogrammetry has been used successfully in traffic management and in traffic accident investigations. One advantage of its use in the latter area is that photographs overlook nothing that may be needed later to reconstruct the accident, and it is possible to restore normal traffic flow quickly.

Even in the field of medicine and dentistry, measurements from X-ray and other photographs and Images have been useful in diagnosis and treatment as shown in figure (2-10).

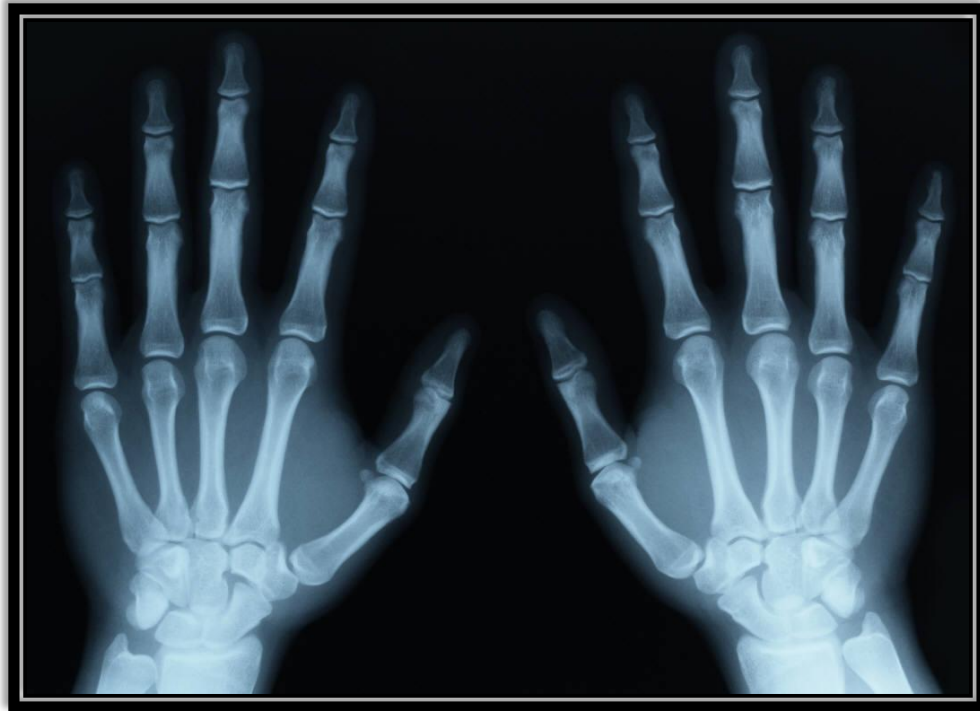


Figure (2 - 10) X-ray photo . [14]

CHAPTER THREE

CLOSE RANGE PHOTOGRAMMETRY

- 3.1 Introduction**
- 3.2 Terrestrial Cameras**
- 3.3 Horizontal and Oblique Terrestrial Photos**
- 3.4 Camera Inclination**
- 3.5 Horizontal and Vertical Angle**
- 3.6 Camera axis and exposure station position**
- 3.7 Location points by intersection from two photos**
- 3.8 Analytical solution for close range photogrammetry**

3.1 Introduction

Terrestrial photogrammetry is an important branch of the science of photogrammetry. It deals with photographs taken with cameras located on the surface of the earth. The cameras may be handheld, mounted on tripods, or suspended from towers or other specially designed mounts. The term close range photogrammetry is generally used for terrestrial photographs having object distances up to 300m. With terrestrial photography, the cameras are usually accessible. So that, direct measurements can be made to obtain exposure station positions similar to airborne GPS control with aerial photography. With some terrestrial cameras, angular orientation can also be measured or set to fixed values, (camera position and tilt angles), so that all elements of exterior orientation of a terrestrial photo are commonly known and do not need be calculated. These exterior orientation parameters are the source of control for the terrestrial photos, which replace in whole or in part the necessity for locating control points in the object space on the photographs.

Terrestrial photography may be static (photos of stationary objects) or dynamic (photos of moving objects). For static photography, slow, fine-grained, high resolution films or digital sensors may be used and the pictures taken with long exposure times. Stereopairs can be obtained by using a single camera and making exposures at both ends of a baseline. In taking dynamic terrestrial photos, fast films or digital sensors to be used with rapid shutter speeds. If Stereopairs of dynamic occurrences are required, two cameras located at the ends of a baseline must make simultaneous exposures, which requires time synchronization capabilities.

3.2 Terrestrial Cameras

A variety of cameras are used in terrestrial photography. All fall into one of two general classifications:

- Metric cameras: for photogrammetric applications. They have fiducial marks in case of analog cameras. They are completely calibrated before their use. Their

calibration values for focal length, principal- point coordinates, and lens distortions can be applied with confidence over long periods.

- Non-metric cameras: manufactured for amateur or professional photograph) where pictorial quality is important but geometric accuracy requirements are generally not considered paramount.

A phototheodolite is an instrument that incorporates a metric camera with a surveyor's theodolite. With this instrument, precise establishment of the direction of the optical axis can be made as shown in Figure (3 - 1).

A stereometric camera system consists of two identical metric cameras which are mounted at the ends of a bar of known length. The optical axes of the cameras are oriented perpendicular to the bar and parallel with each other. The length of the bar provides a known baseline length between the cameras, which is important for controlling scale as shown in Figure (3 - 2).

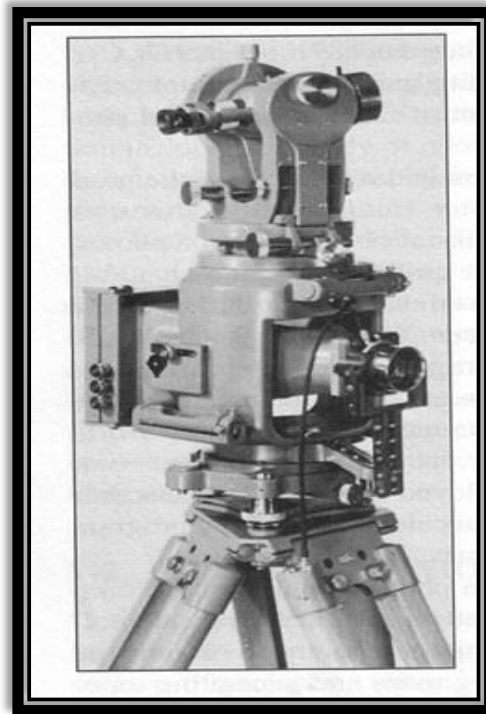


Figure (3 - 1) phototheodolite . [2]



Figure (3 - 2) stereometric camera system . [2].

3.3 Horizontal and Oblique Terrestrial Photos

Terrestrial photos may be classified according to their inclination from the horizontal axis into horizontal or oblique. This classification defines the orientation of the camera axis at the time of the photography.

- 3.3.1 Horizontal terrestrial photos: if the camera axis is horizontal when the exposure is made. The plane of the photo is vertical. So if metric camera is used the x-axis is horizontal and the y-axis is vertical, as shown in figure (3-3).
- 3.3.2 Oblique terrestrial photo: the camera axis is inclined either up or down in an angle θ from horizontal. If θ is upward is called elevation angle. If its downward it called depressing angle as shown in figure (3-4).

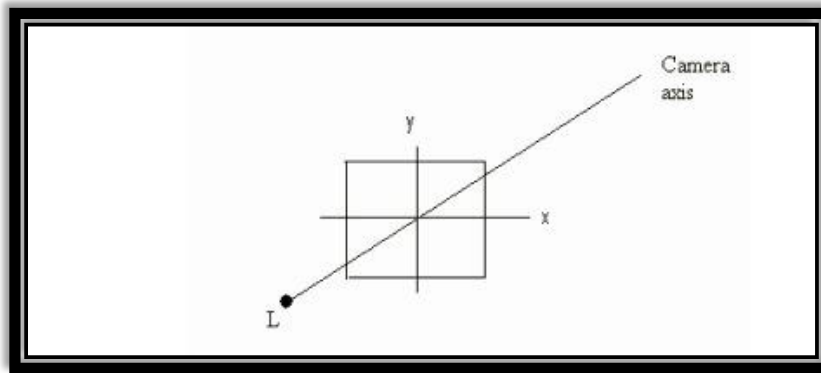


Figure (3 - 3) Camera axis . [1]

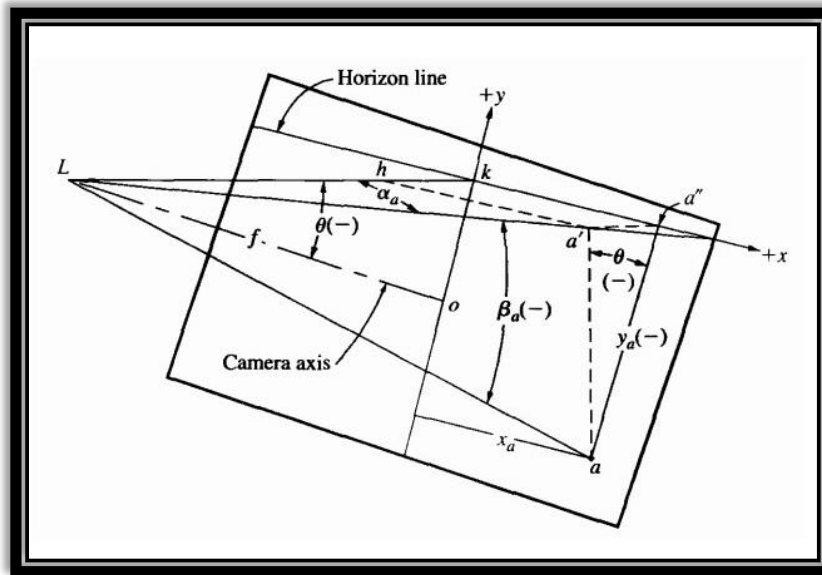


Figure (3 - 4) Horizontal and vertical angles from measurements on an oblique terrestrial photo . [1]

3.4 Camera Inclination

Determining the angle of inclination of the camera axis of a terrestrial photo is defined based on the following three basic principles of perspective geometry as shown in figure (3-5):

1. Horizontal parallel lines intersect at a vanishing point on the horizon v.
2. Vertical parallel lines intersect at the nadir (or zenith) n.

3. The line from n through the principal point o intersects the horizon at a right angle at point k .

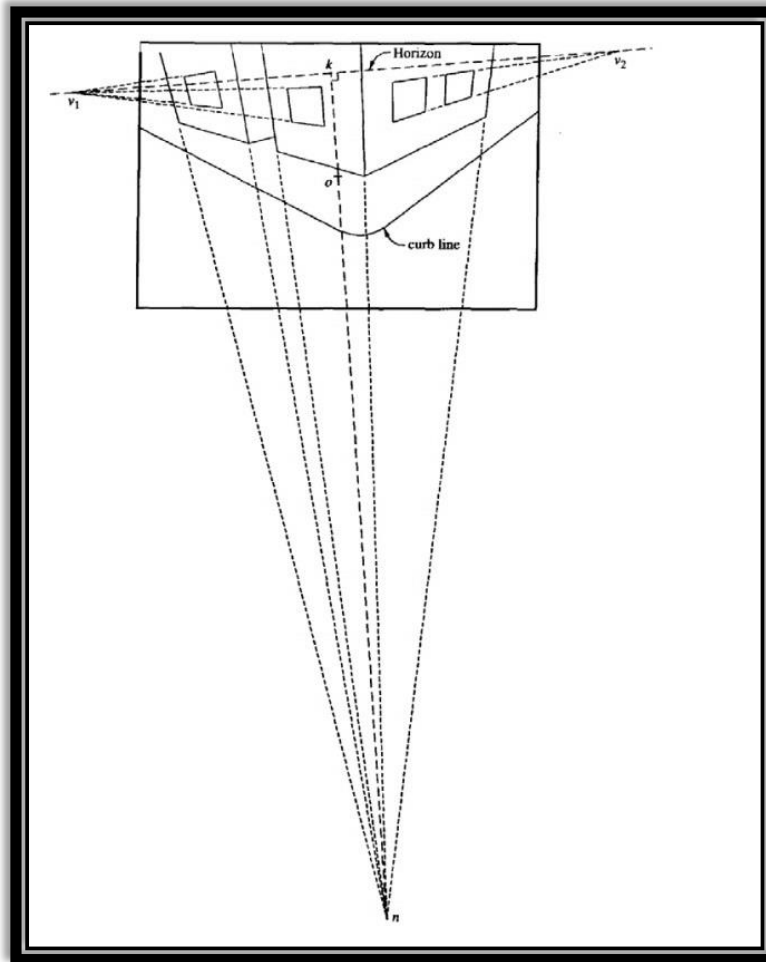


Figure (3 - 5) Location of horizon and nadir on an oblique photograph . [1]

The photo coordinates system can be established as shown in figure (3-6) , where:

1. The origin is k .
2. The x-axis is positive in the right side of the origin in the horizon line (V_1V_2 as shown in figure (3-5))
3. The y-axis is positive perpendicularly to x-axis upwards passing through the principle point o and the origin k .

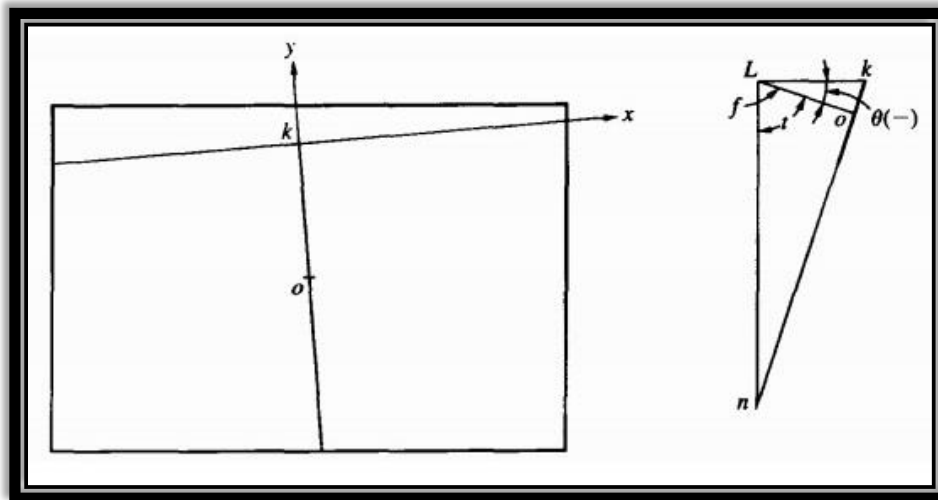


Figure (3 - 6) oblique photo coordinate axis system . [1]

There are two ways to determine the depression angle, the first way is reading:

$$\theta = \tan\left(\frac{y}{f}\right) \tag{3.1}$$

$$y = ko \tag{3.2}$$

The angle θ is depression angle, if $y = ko$ is negative in figure (3-6), else it is an elevation angle.

The second way to determine the depression angle, is using the angle t in figure (3-6), where t reads:

$$t = \tan^{-1}\left(\frac{on}{f}\right) \tag{3.3}$$

Then, the depression angle is given by

$$\theta = t - 90^\circ \tag{3.4}$$

If θ is elevation angle, the θ reads

$$\theta = 90^\circ - \tan^{-1}\left(\frac{oz}{f}\right) \tag{3.5}$$

3.5 Measuring Horizontal and Vertical Angles

Horizontal angle α between the vertical planes, ($La'a$) as shown in the figure (3-7) , containing image point a and the vertical plane, (Lko), containing the camera axis is:

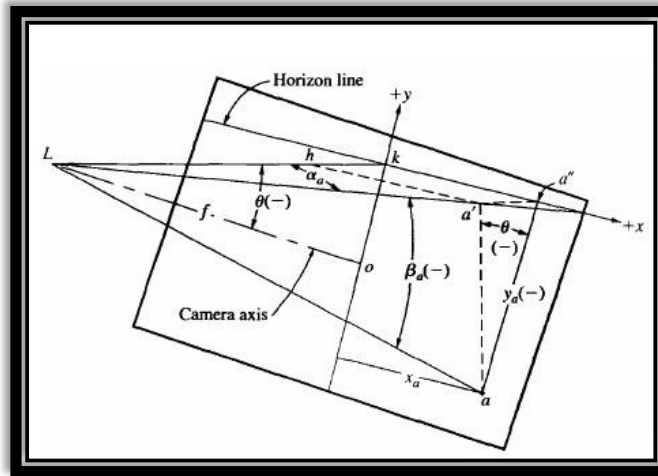


Figure (3 - 7) Horizontal and vertical angles from measurements on an oblique terrestrial photo . [1]

$$\alpha_a = \tan^{-1} \left(\frac{x_a}{f \sec \theta - y_a \sin \theta} \right) \tag{3.6}$$

α is positive if it is clockwise, and negative if it is counter clockwise.

Vertical angle β to image point a , as shown in figure (3-8) can be calculated from the following equation:

$$\beta_a = \tan^{-1} \left(\frac{aa'}{La'} \right) \tag{3.7a}$$

$$La' = (Lk - hk) \sec \alpha_a \tag{3.7b}$$

$$\beta_a = \tan^{-1} \left[\frac{aa'}{(Lk - hk) \sec \alpha_a} \right] \tag{3.7c}$$

$$\beta_a = \tan^{-1} \left[\frac{y_a \cos \theta}{(f \sec \theta - y_a \sin \theta) \sec \alpha_a} \right] \tag{3.7d}$$

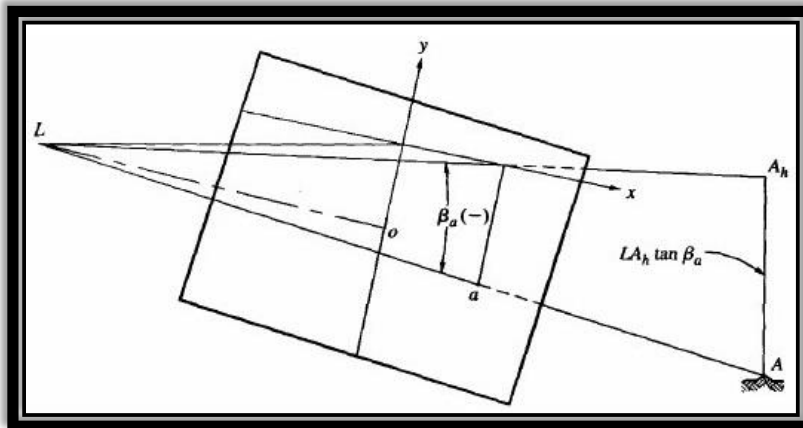


Figure (3 - 8) Determining elevation of camera station of terrestrial photo by using one vertical control point . [1]

3.6 Camera axis and exposure station position

The method as explained in figure (3-9) is called three point resection, which is used to determine the exposure station position.

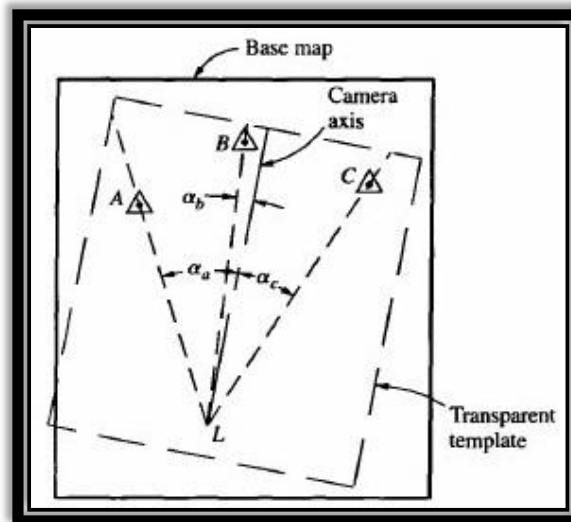


Figure (3 - 9) Graphical three point resection to locate exposure station and direction of optical axis . [1]

The following steps are done to find the exposure position:

1. Three known points horizontal positions (A,B,C) drawn to scale on a map plate.

2. θ has to be known.
3. The angles between the three points have to be calculated.
4. Graphical three-point resection procedure, using transparent template containing the three rays and the camera axis.
5. The template is placed on the base map and adjusted in position and rotation until the three rays simultaneously pass through their respective plotted control points.
6. the position of L is fixed according to the map coordinates system.

By another method, the position of L can be calculated resection problem numerically, as in surveying. The elevation of the exposure station is the height of the camera lens above the datum. Assume that the position and elevation of point A are known as shown in figure(3-8). And $(a \beta)$ is calculated as follows:

$$Elev L = elev A - LA_h \tan \beta_a \quad (3.8)$$

3.7 Calculation of points position

If images of an object point appear in two or more oblique photos, the position and elevation of the point can readily be determined, provided the camera positions and directions of the optical axis are known. Figure (3-10) illustrates two oblique photos taken from exposure stations L and L' . And Figure (3-11) show Plan view of intersection from two oblique terrestrial photos.

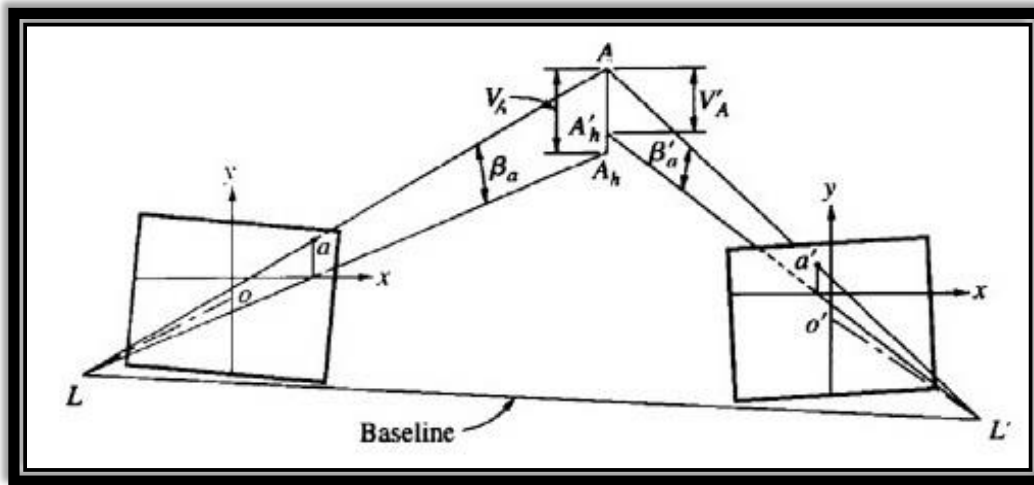


Figure (3 - 10) Locating points by intersection from two oblique terrestrial photos . [1]

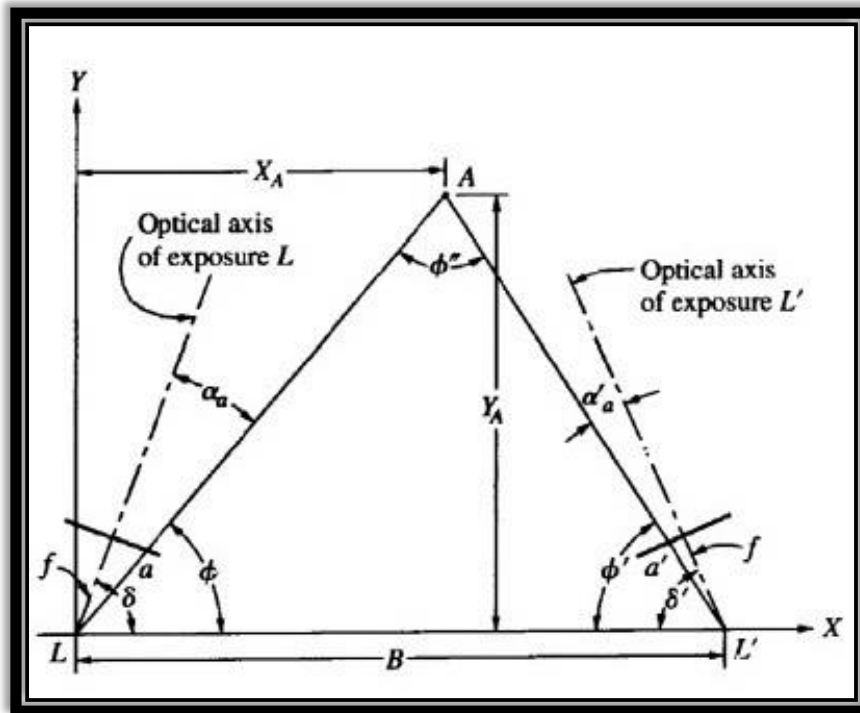


Figure (3 - 11) Plan view of intersection from two oblique terrestrial photos . [1]

δ and δ' can be determined by three points resection.
 α, α', β , and β' can be calculated as explained before.
 Then the position of a point A is calculated as follows:

$$\phi' = \delta' + \alpha'_a \quad (3.9)$$

$$\phi'' = 180^\circ - \phi - \phi' \quad (3.10)$$

$$LA = \frac{B \sin \phi'}{\sin \phi''} \quad (3.11)$$

$$L'A = \frac{B \sin \phi}{\sin \phi''} \quad (3.12)$$

$$X_A = LA \cos \phi \quad (3.13)$$

$$Y_A = LA \sin \phi \quad (3.14)$$

$$X_A = B - L'A \cos \phi' \quad (3.15)$$

$$Y_A = L'A \sin \phi' \quad (3.16)$$

$$Elev A = elev L + V_A \quad (3.17)$$

$$V_A = LA_h \tan \beta_{a'} \quad (3.18)$$

$$Elev A = elev L' + V'_A \quad (3.19)$$

$$V'_A = L'A'_h \tan \beta'_{a'} \quad (3.20)$$

3.8 Analytical solution for close range photogrammetry

The analytical solution for close range photogrammetry can be applied using the same methods in aerial photogrammetry, and this need the following steps:

1. Interior orientation using affine coordinates transformations, we get xy coordinates in the fiducial coordinates system.
2. Relative Orientation using collinearity equations, we get model coordinates.
3. Absolute Orientation using 3D conformal coordinates transformations to get the ground coordinates East, North and Elevations (E,N,H)

It must be noted that: in the relative orientation, the X-axis is in the base between the exposure stations. And the Z-axis is the line Vertical to the image plane. The Y-axis is perpendicular to the XZ-plane, positive upwards. See figure (3-12).

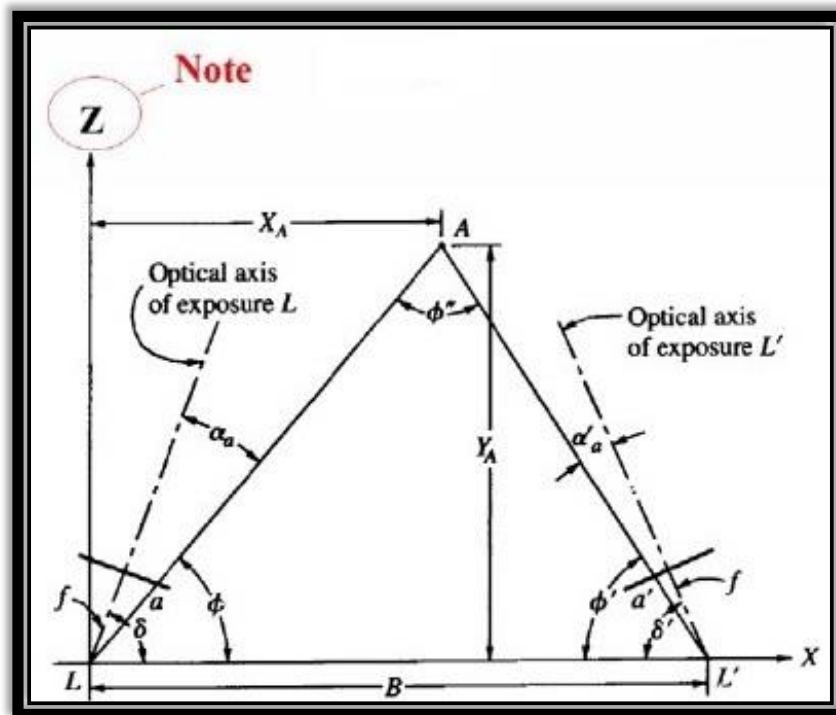


Figure (3 - 12) . [1]

CHAPTER FOUR

APPLICATIONS OF CLOSE RANGE PHOTOGRAMMETRY

- 4.1 Introduction**
- 4.2 Accident reconstruction**
- 4.3 Crime Scene**
- 4.4 Structural Analysis**
- 4.5 Volume Computing**
- 4.6 Facial Recognition**
- 4.7 Documentation of Cultural (Fatih Mosque):**

4.1 Introduction

There are a lot of applications in close range photogrammetry that used in all fields of life close range photogrammetry can be used instead of using traditional methods of survey in some areas. Here, we introduce some applications of close range photogrammetry specify accident reconstruction, crime scene, structural analysis, volume computing, facial recognition, and documentation of cultural (Fatih Mosque):

4.2 Accident reconstruction

The aim of traffic accident reconstruction (AR) is, as the name implies, to reconstruct motor vehicle collision scenes. Whether the final requirements of the AR process are to assist in calculations (such as vehicle speed), to analyze the dynamics of the collision event(s) , as shown in figure (4-1).

For most scenes, it's a low-cost, fast and accurate method of permanently archiving & mapping critical scene evidence in 3D. Improves safety, less time on road, Easy to use (the photogrammetry software does all the 'math' automatically)

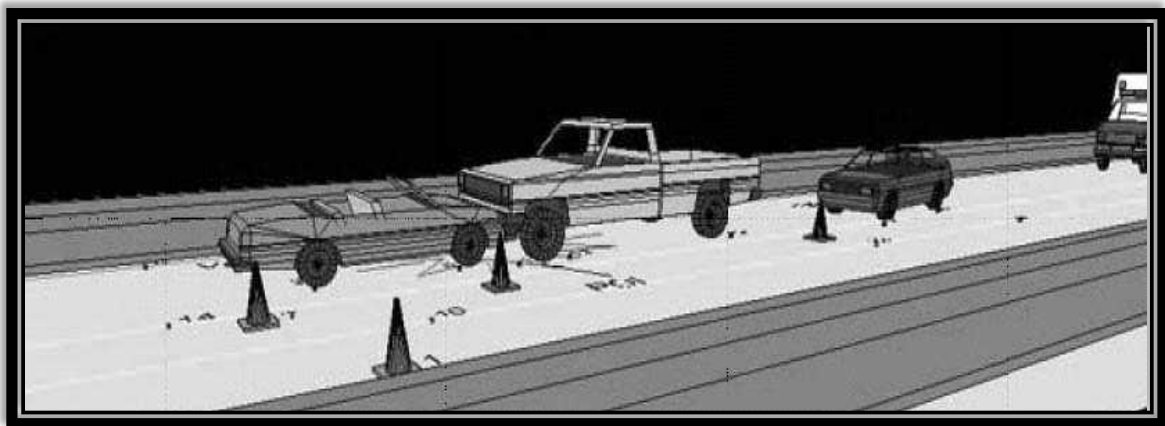


Figure (4 - 1) Analyze the dynamics of the collision event . [3]

4.3 Crime Scene

The aim of crime scene measurement is to reconstruct the real-world incident into a scaled diagram, represented as a 3-D model used for visualization and animation. Whether final requirements of the measurements are to assist in the determination of a suspect's location, bullet trajectory, blood spatter, weapons location, drugs, or a myriad of other criminal factors, the initial step is to accurately characterize the dimensions of the incident scene. The comprehensiveness of the model required can vary depending upon the use of the 'mapping' data produced. For example, in the case of measuring a crime scene involving bullet trajectory, the bullet path may have traveled through two or more adjacent rooms, and an accurate 3-D model is beneficial in order to document the precise bullet flight path through the rooms. The ability to use non-contact measurement methods is highly attractive when combining the recording of e.g., bullet trajectory, blood spatter, blood pool areas and other bio-hazard conditions - (such as the documentation and recording of meth labs). Conversely, in some crime scenes, a simple measurement of evidence using more traditional measurement approaches may suffice for the needs of the investigator's diagram.

It is called "Close-Range Photogrammetry." With this technology, 3D measurements can be extrapolated from 2D digital camera images acquired from various angles at the scene. In such cases, a digital camera can be used to quickly capture the necessary scene details and evidence. Later, a skilled person can calculate measurements based on the scene's digital images , as shown in figure (4-2).



Figure (4 - 2) Example of images of crime scene . [4]

4.4 Structural Analysis

Dimensional surveys of structural features are generally required to document existing conditions for engineering analysis and planning. Traditionally, survey crews obtain measurements using conventional equipment and methods, which involve physically placing measurement devices on every key feature. Safety was also a critical issue - traditional methodology dictated that a person climb upon each of the four suspension cables to the two bridge towers. Use digital close-range photogrammetry to measure structural features with high accuracy, increased safety, and minimal impact on traffic flow.

Photogrammetric techniques, measuring objects from photographs, have been utilized since the late 1800s. Close-range photogrammetry is a technique for accurately

measuring objects directly from photographs or digital images captured with a camera at close range. Multiple, overlapping images taken from different perspectives, produces measurements that can be used to create accurate as-built 3D models. Knowing the position of camera is not necessary because the geometry of the object is established directly from the images.

Compared to traditional surveying methods, this measurement approach was efficient and rapid, significantly reducing the time required to collect data in the field. Measurements collected in less than three days in the field would have taken 10 days in a conventional survey. Second, it was considerably safer. Third, the method was non-intrusive, creating minimal impact on traffic flow. Finally, the process produced a comprehensive visual record of existing site conditions from which any identifiable features can be measured or geometrically assessed at a later date. The same process can be used to obtain dimensional measurements efficiently on inaccessible structures such as tunnels and dams, and large or complex facilities such as refineries or water treatment plants. The acquired data is infinite and the cost savings substantial, as shown in figure (4-3).

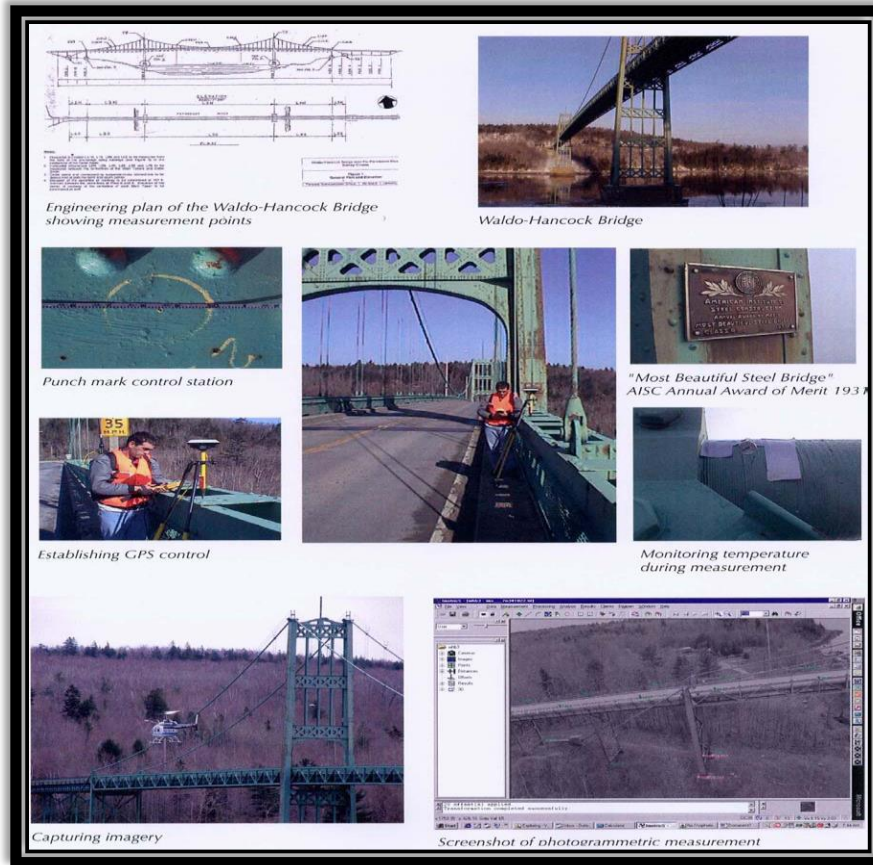


Figure (4 - 3) Close-Range Photogrammetric Measurement for Structural Analysis . [5]

4.5 Volume Computing

The purpose of introducing close range photogrammetry method in excavated volume estimation is to increase efficiencies of the estimation processes as well as the reliability of the result. A study is to be done in laboratory to investigate the applicability of the photogrammetry in estimating the excavated volume of soil or rock slope using a physical model. The physical model assembles the actual slope condition. Photogrammetry procedures were set up to determine the volume of the excavated materials. Then, a simple verification test is done to verify the result using close-range photogrammetry. Comparison between close-range photogrammetry and conventional methods will also be discussed to prove that close-range photogrammetry can be used as one of the reliable methods in estimation of excavated materials.

Volume calculation and estimation in rock mass serves a wide range of purposes. One of the main purposes is to obtain the quantities of excavation, and filling as well as other earthworks activities. This quantity will be later included into a schedule or bill of quantities which is to be stated in the contract. The volume obtained will also be reviewed for the purpose of payment at the later stage of the project. Early acknowledgement of the volume of excavation at a proposed site will also help engineers and project manager to proceed with designing works, such as determining suitable formation levels. Thus, estimating overall embankments or excavation required for the site.

The study area is a sand heap Figure (4-4). A truck was used to calculate volume of the sand.

Because dimensions of the truck can be measure easily. The shape of the truck is rectangular

prism. Width, length and height are sufficient to volume calculation. Volume of the truck body

has been calculated as 17.4375 m^3 sand excavated and loaded to the truck. 5 truck sand have

been excavated. The compression ratio of the sand has been calculated as %10. 78.4688 m^3

sand have been excavated of the study area.

Control targets have been placed before the excavation of study area Figure (4-4) Local 3 dimensional coordinates have been measured using a electronic reflector less total station. Photographs of the excavation area have been taken by digital camera. Later, 5 truck body sand have been excavated and converged. Control targets have been placed again Figure (4-5) coordinates of the targets have been measured after the excavation. Photographs of the excavation area have been taken again after the excavation. Control target coordinates and photographs have been transferred to the software. Photogrammetric evaluations have been completed. 616 field points have been measured for the non-excavated area. 569 field points have been measured after the excavation

Obtained coordinate values transferred to the surfer software. Volume of the excavation has been calculated from two surface differences as 74.972 m^3 .



Figure (4 - 4) Study area . [6]

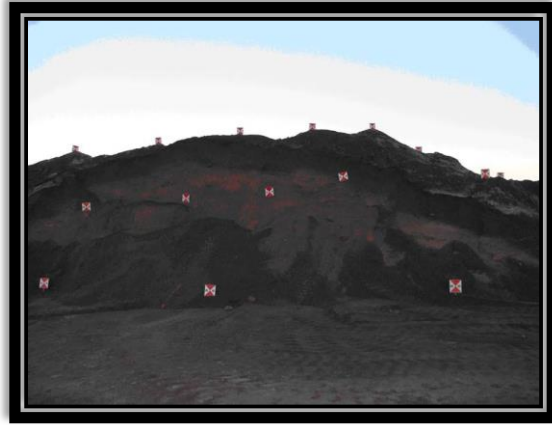


Figure (4 - 5) Post Excavation . [6]

4.6 Facial Recognition

close range photogrammetry with overlapping photographs were used to create a three dimensional model of human face where coordinates of selected object points were extracted and used to calculate five different geometric quantities that been used as biometric authentication for uniquely recognizing humans. Then , the probabilistic neural networks, with their remarkable ability to derive meaning from complicated or imprecise data, utilize the extracted geometric quantities to find patterns and detect trends that are too complex to be noticed by either humans or other computer techniques. Quantifiable dimensions that based on geometric attributes rather than radiometric characteristics has been successfully extracted using close range photogrammetry. the Probabilistic Neural Network (PNN) as a kind from radial basis network group has been used to specify a geometrics parameters for face recognition where the designed recognition method is not effected by face gesture or color and has lower cost compared with other techniques.

This method is reliable and flexible with respect to the level of detail that describe the human surface. Experimental results using real data proved the feasibility and the quality of the suggested approach.

Tacking multiple Stereo images all-around the object (human Face) with overlapping ranges from 75-100%. For each object six images has been captured. Three positions of the camera were adopted with almost the same distant between the camera and the object. First position directly in front of the target, the second and third position at angle approximately 45 degree at the right and left direction, Figure (2-6). Two images were taken from each position (portrait and landscape).





Figure (4 - 6) Image capturing based on three different positions . [7]

Marking and referencing: This stage includes measuring the interest point (marking) and referencing as well as implementation of bundle adjustment model to extract the three dimensional coordinates of conjugate points. The photogrammetric process starts with marking that tend to place and identify the required points on the face picture. Figure (2-7) shows the interest points on the face target which consist of:

- Eye terminal-points
- Upper middle sections of eye sockets
- Nose-top point
- Mouth terminal-points
- Lower chin point

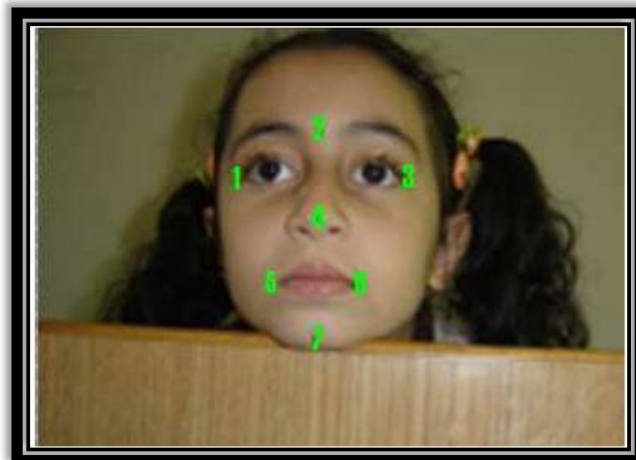


Figure (4 - 7) Interest points of the face ... [7]

The relative orientation can be performed by measuring at least five tie points in each stereo-pair. In this work seven points were selected as shown in Figure (2-7). It has to be clear that exact points would increase the accuracy and enhance the solutions as the number used to solve unknown parameters in the least square adjustment increase. It has to be mentioned that the 3D coordinates of the mentioned tie points (1, 2, 3, 4, 7) would allow for extracting relational attributes of the face rather than radiometric attributes. Recognition that relies on geometric attributes does not get affected by the face gesture (sad, happy...), motion of the face, motion of the face itself, the color of skin (color of skin varies for the same person), existence or absence of sunglasses, lenses, or any other face features that may change from time to time.

4.7 Documentation of Cultural (Fatih Mosque)

Conservation of historical buildings and constructions, being important parts of cultural heritage, determining the historical buildings facades is one of the main operations. Historical buildings are usually characterized by irregular geometry, very complex surface. In this context, close range photogrammetry is inevitable and has been used successfully for documentation of cultural heritage for many years.

Digital close range photogrammetry is currently an effective system providing both vector and raster data type. This method is also allowing metric-morphological reconstruction of cultural heritage.

CHAPTER FIVE

CAMERA CALIBRATION

- 5.1 Introduction**
- 5.2 Elements of Interior Orientation**
- 5.3 Laboratory Methods of Camera Calibration**
- 5.4 Stellar Methods**
- 5.5 Field Methods**
- 5.6 Analytical Self Calibration**
- 5.7 Automatic Camera Calibration**
- 5.8 Computation Of Self Calibration**
- 5.9 Test Field**
- 5.10 Zoom Dependent Camera Calibration**
- 5.11 Z-D Calibration Model**

5.1 Introduction

Camera calibration has been applied in different photogrammetric application and methods for several decades. A general definition of calibration by the International Vocabulary of Basic and General Terms in Metrology (VIM) is “set of operations that establish, under specified conditions, the relationship between values of quantities indicated by a measuring instrument or measuring system, or values represented by a material measure or a reference material, and the corresponding values realized by standards”.

Another definition, for photogrammetric camera calibration, was given as calibration is “the act and process of determining certain specific measurements in a camera or other instrument or device by comparison with a standard, for use in correcting or compensating errors for purposes of record”.

After it’s production and before it’s use, aerial cameras must be carefully calibrated to determine precise and accurate values for a number of variables. These variables, generally referred to as the elements of interior orientation, are needed so that accurate spatial information can be determined precisely from photographs with correct geometry.

In general, camera calibration methods may be classified into one of three basic categories:

1. Laboratory methods.
2. Field methods.
3. Stellar methods.

Of these, laboratory methods are most frequently utilized and are normally performed by either camera manufacturers or agencies of the federal government. In one particular method of laboratory calibration, which uses a multicollimator, as well as in the field and stellar procedures, the general approach consists of photographing an array of targets whose relative positions are accurately known. Elements of interior orientation are then determined by making precise measurements of the target images and comparing their actual image locations with the positions they should have occupied had the camera

produced a perfect perspective view. In another laboratory method, which employs a goniometer, direct measurements are made of projections through the camera lens of precisely positioned grid points located in the camera focal plane. Comparisons are then made with what the true projections should have been.

5.2 Elements of Interior Orientation

The elements of interior orientation which can be determined through camera calibration are: calibrated focal length (CFL), Symmetric radial lens distortion, Decentering lens distortion, Principal point location and Fiducial mark coordinates.

5.2.1 Calibrated focal length (CFL): This is the focal length that produces an overall mean distribution of lens distortion. Actually this parameter would be better termed calibrated principal distance since it represents the distance from the rear nodal point of the lens to the principal point of the photograph. When aerial mapping cameras are manufactured, this distance is set to correspond to the optical focal length of the lens as nearly as possible, hence the more common, though somewhat misleading, term calibrated focal length.

5.2.2 Symmetric radial lens distortion: This is the symmetric component of distortion that occurs along radial lines from the principal point. Although the amount may be negligible, this type of distortion is theoretically always present even if the lens system is perfectly manufactured to design specifications. Figure(5-1) shows a typical symmetric radial lens distortion pattern with magnitudes of distortion greatly exaggerated. Notice that distortion occurs in a direction inward toward, or outward from, the center of the image.

5.2.3 Decentering lens distortion: This is the lens distortion that remains after compensation for symmetric radial lens distortion. Decentering distortion can be further broken down into asymmetric radial and tangential lens distortion components. These distortions are caused by imperfections in the manufacture and alignment of the lens system. Figure(5-2) shows a typical decentering

distortion pattern, again with the magnitudes greatly exaggerated. Figure(5-3) shows a typical pattern of combined symmetric radial and decentering distortion.

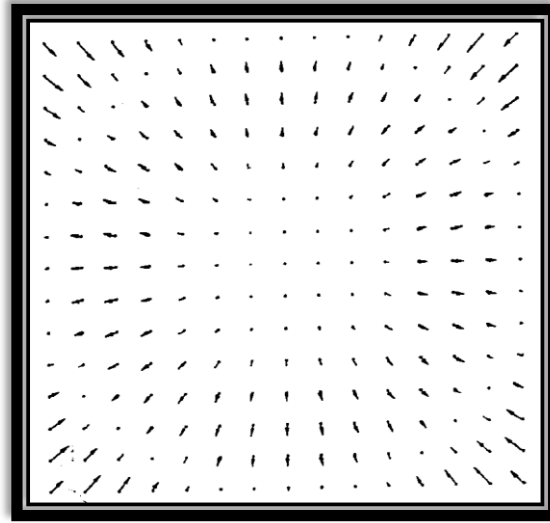


Figure (5 - 1) Typical symmetric radial lens . [1]

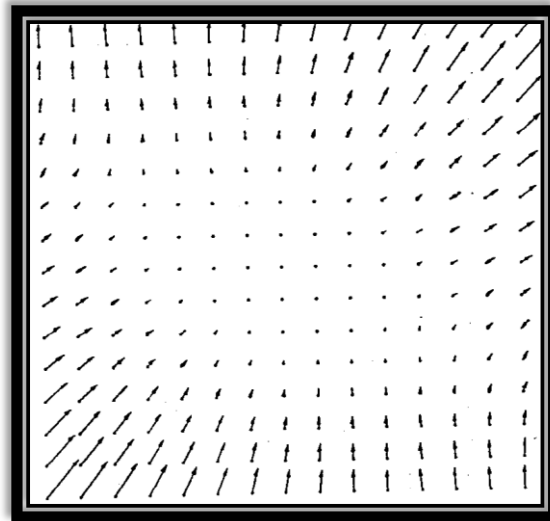


Figure (5 - 2) Typical decentering distortion . [1]

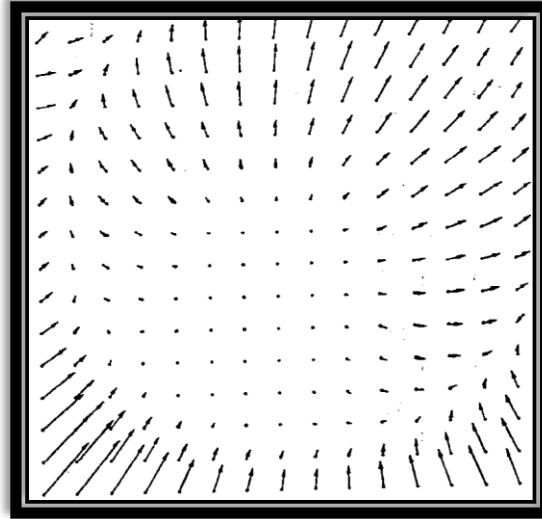


Figure (5 - 3) combined symmetric radial and decentering distortion . [1]

5.2.4 Principal point location: This is specified by coordinates of the principal point given with respect to the x and y coordinates of the fiducial marks. Although it is the intent in camera manufacture to place the fiducial marks so that lines between opposite pairs intersect at the principal point, there is always some small deviation from this ideal condition.

5.2.5 Fiducial mark coordinates: These are the x and y coordinates of the fiducial marks which provide the two-dimensional positional reference for the principal point as well as images on the photograph.

5.3 Laboratory Methods of Camera Calibration

Laboratory calibration is generally used only for metric cameras. The IO parameters are determined by goniometers, multicollimator.

The multicollimator method consists of photographing, onto a glass plate, images projected through a number of individual collimators mounted in a precisely measured angular array. A single collimator consists of a lens with a cross mounted in its plane of infinite focus. Therefore, light rays carrying the image of the cross are projected through the collimator lens and emerge parallel. When these light rays are directed toward the

lens of an aerial camera, the cross will be perfectly imaged on the camera's focal plane because aerial cameras are focused for parallel light rays. One plane of collimators is illustrated in figure (5-4). The individual collimators are rigidly mounted so that the optical axes of adjacent collimators intersect at known measured angles.

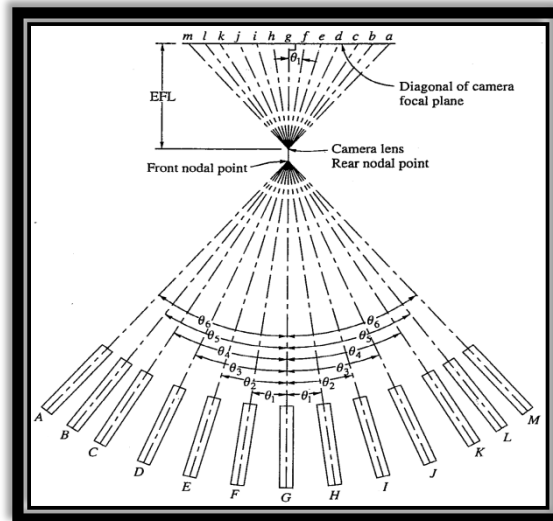


Figure (5 - 4) 13 collimators for camera calibration . [1]

5.4 Stellar methods

In the stellar method, a target array consisting of identifiable stars is photographed, and the instant of exposure is recorded. Right ascensions and declinations of the stars can be obtained from an ephemeris for the precise instant of exposure so that the angles subtended by the stars at the camera station become known. Then these are compared to the angles obtained from precise measurements of the imaged stars. A drawback of this method is that since the rays of light from the stars pass through the atmosphere, compensation must be made for atmospheric refraction. On the other hand, there will be a large number of stars distributed throughout the camera format, enabling a more precise determination of lens distortion parameters.

5.5 Field methods

Field procedures require that an array of targets be established and that their positions with respect to the camera station be measured precisely and accurately in three dimensions. This can be achieved conveniently using GPS methods. The targets are placed far enough from the camera station so that there is no noticeable image degradation. Recall that an aerial camera is fixed for infinite focus. In this configuration, the camera must be placed in a special apparatus such as a fixed tower, so that camera station coordinates are correctly related to target coordinates. This enables the CFL (Calibrated Focal Length) and principal point location to be determined as well as lens distortion parameters, even if the target configuration is essentially a two-dimensional plane. If the targets are well distributed in depth as well as laterally, accurate location of the camera is less important.

5.6 Analytical Self Calibration

Analytical self-calibration is a computational process wherein camera calibration parameters are included in the photogrammetric solution, generally in a combined interior, relative and absolute orientation. The process uses collinearity equations that have been augmented with additional terms to account for adjustment of the calibrated focal length, principal point offsets, and symmetric radial and decentering lens distortion.

In addition, the equations might include corrections for atmospheric refraction. The common form of the augmented collinearity equations is given as:

$$x_a = x_o - x'_a(k_1 r_a^2 + k_2 r_a^4 + k_3 r_a^6) - (1 + p_3^2 r_a^2) \left[p_1 (3x_a'^2 + y_a'^2) + 2p_2 x'_a y'_a \right] - f \frac{r}{q} \quad (5.1)$$

$$y_a = y_o - y'_a(k_1 r_a^2 + k_2 r_a^4 + k_3 r_a^6) - (1 + p_3^2 r_a^2) \left[2p_1 x'_a y'_a + p_2 (x_a'^2 + 3y_a'^2) \right] - f \frac{s}{q} \quad (5.2)$$

Where x_a, y_a = measured photo coordinates related to fiducials

x_o, y_o = coordinates of the principal point

k_1, k_2, k_3 = symmetric radial lens distortion coefficients

p_1, p_2, p_3 = decentering distortion coefficients

f = calibrated focal length

r, s, q = collinearity equation terms

$$x'_a = x_a - x_0 \quad (5.3)$$

$$y'_a = y_a - y_0 \quad (5.4)$$

$$r_a^2 = x_a'^2 - y_a'^2 \quad (5.5)$$

$$q = m_{31}(X_A - X_L) + m_{32}(Y_A - Y_L) + m_{33}(Z_A - Z_L) \quad (5.6)$$

$$r = m_{11}(X_A - X_L) + m_{12}(Y_A - Y_L) + m_{13}(Z_A - Z_L) \quad (5.7)$$

$$s = m_{21}(X_A - X_L) + m_{22}(Y_A - Y_L) + m_{23}(Z_A - Z_L) \quad (5.8)$$

Where

$$m_{11} = \cos \omega \cos \phi \cos k \quad (5.9)$$

$$m_{12} = \sin \omega \sin \phi \cos k + \cos \omega \sin k \quad (5.10)$$

$$m_{13} = -\cos \omega \sin \phi \cos k + \sin \omega \sin k \quad (5.11)$$

$$m_{21} = -\cos \phi \sin k \quad (5.12)$$

$$m_{22} = -\sin \omega \sin \phi \sin k + \cos \omega \cos k \quad (5.13)$$

$$m_{23} = \cos \omega \sin \phi \sin k + \sin \omega \cos k \quad (5.14)$$

$$m_{31} = \sin \phi \quad (5.15)$$

$$m_{32} = -\sin \omega \cos \phi \quad (5.16)$$

$$m_{33} = \cos \omega \cos \phi \quad (5.17)$$

Where ω, ϕ, k = rotational angles

5.7 Automatic Camera Calibration

The implementation of an automatic camera calibration system should consist of two stages:

1. Image processing: detecting targets, positioning target centers, and identify target numbers.
2. Computation of self-calibration: initial value estimation and bundle adjustment.

More than 50 artificial targets are generally needed for a camera calibration task. Due to their similarity, targets tend to be mismatched or misidentified among a set of images. For automatic target identification and for users being able to verify the results, coded targets are preferable to the implementation of automatic camera calibration. A coded target should meet the requirements below:

1. Independence of location, rotation and scale.
2. Precise and accurate center point determination.
3. Detection and localization in any patterned image without initial values
4. Short processing time
5. Compact target size
6. A low rate of manufacturing costs

Self-calibration is an extension of the bundle adjustment. It simultaneously solves the calibration parameters and points coordinates in object space with the measurements of a sufficient number of well-distributed points. Thus, the major problem of automatic self-calibration is how to estimate the initial value. Some research use additional equipments, such as the Inertial System (INS), to provide the position and the attitude of a camera. Some others use 3 object space control points and the closed-form space resection to estimate the initial values of orientation parameters. In this paper, the initial coordinates of targets are derived from the previous photogrammetric task, or simply measured by meters.

5.8 Computation Of Self Calibration

Self-calibration technique does not require any object space control as a means of camera calibration. The observations of targets are used as the data required for both object points determination and for the determination of camera calibration parameters. The basic formulas of self-calibration are the collinearity equations with lens distortion and a series of additional parameters (APs), which can be written as:

$$x_{ij} - x_p + \frac{(x_{ij} - x_p)}{r} \delta_r + \Delta x = f_i^x \frac{(X_j - X_i^\circ)m_{11} + (Y_j - Y_i^\circ)m_{12} + (Z_j - Z_i^\circ)m_{13}}{(X_j - X_i^\circ)m_{31} + (Y_j - Y_i^\circ)m_{32} + (Z_j - Z_i^\circ)m_{33}} + dx_{AP} \quad (5.18)$$

$$y_{ij} - y_p + \frac{(y_{ij} - y_p)}{r} \delta_r + \Delta y = f_i^y \frac{(X_j - X_i^\circ)m_{21} + (Y_j - Y_i^\circ)m_{22} + (Z_j - Z_i^\circ)m_{23}}{(X_j - X_i^\circ)m_{31} + (Y_j - Y_i^\circ)m_{32} + (Z_j - Z_i^\circ)m_{33}} + dy_{AP} \quad (5.19)$$

Where \circ : the perspective center

i : the i th photograph

p : the principle point

j : the j th point

In equation (1), δ_r represents the radial distortion and Δx , Δy represent the decentering distortions. On the right side of the equation, f_i^x , f_i^y are the principle distances from the image respect to x and y . These two factors are usually simplified as a common value f_i . The terms m_{11} , m_{12} , ..., m_{13} are elements of the rotation matrix, which consists of three

rotation angle: ω , ϕ , κ . The last terms dx_{AP} and dy_{AP} are additional parameters modeled with polynomials. The purpose of the camera calibration is to solve the interior orientation elements: x_p , y_p , f_i , lens distortion parameters δ_r , Δx , Δy ; and the additional parameters dx_{AP} , dy_{AP} . In self-calibration, orientation parameters (m_{11} , m_{12} ... m_{33}) and observed points ground coordinates (X_j , Y_j , Z_j) are solved simultaneously. However, the collinearity equations are nonlinear, so that the Newton-Raphson approach of least squares adjustment is used to solve the unknowns, which is an iteration approach.

5.9 Test Field

The test field applied for the experiments as shown in figure (5-5) is a three dimensional control field. There are 29 targets fixed on the aluminum rods hung on the ceiling or on the walls. The object coordinates of the targets were measured using Wild P32 metric camera. Six photographs were taken to form a solid intersection block. The distribution of exposure stations is shown in figure (5-6). Station 1 and 4 are on the same position but in different heights, so do the station pairs of (2, 5) and (3, 6). The image coordinates of the targets were measured using an analytical plotter.



Figure (5 - 5) The test field . [8]

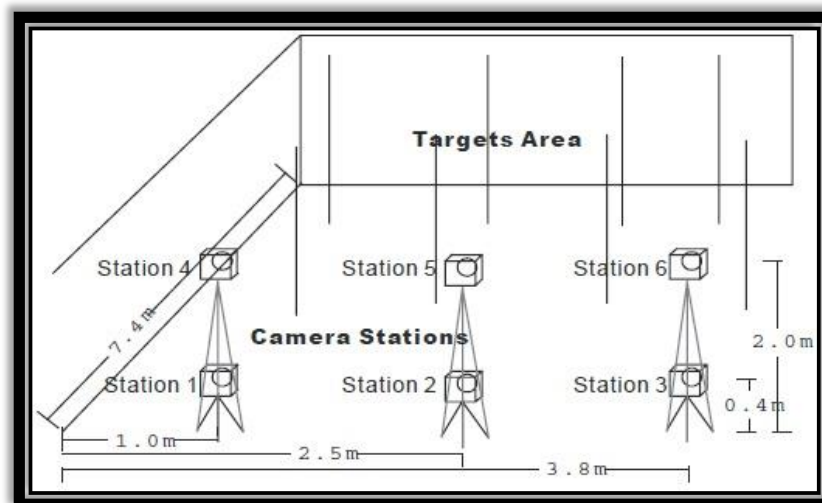


Figure (5 - 6) The distribution of exposure stations . [8]

5.10 Zoom Dependent Camera Calibration

A recently developed process, titled zoom-dependent (Z-D) calibration, removes the necessity for the zoom setting to be fixed during the image capture process. Implementation of Z-D calibration requires that the camera be pre-calibrated at four or more focal settings within the zoom range, nominally at shortest and longest focal lengths, and at two mid-zoom settings. This requirement, coupled with issues of data management in carrying different focal settings for potentially every image within a bundle adjustment, has largely accounted for the reason that Z-D calibration has not previously been implemented within COTS software for close-range photogrammetry.

Cameras employed for photogrammetric measurement have traditionally utilised unifocal lenses where, for a give focus setting, a fixed camera model can be applied. The parameters of this model are well-known: the principal distance, principal point offsets and coefficients of radial and decentring distortion. These parameters are physically interpretable and can fully describe the metric behavior of a camera/lens combination at a specified focal setting to an accuracy of 0.1 pixel and better. In close-range photogrammetry, the recovery of camera parameters is nowadays generally performed via the self calibrating bundle adjustment.

5.11 Z-D Calibration Model

A practical, empirically derived adjustable camera model that characterises the variation of calibration parameters with zoom settings is the following:

$$x^{corr} = x - x_p^{(ci)} + (x - x_p^{(ci)}) K_1^{(ci)} r^2 \quad (5.20)$$

$$y^{corr} = y - y_p^{(ci)} + (y - y_p^{(ci)}) K_1^{(ci)} r^2 \quad (5.21)$$

Here, x and y are the measured image coordinates, x^{corr} and y^{corr} the corrected coordinates and r the radial distance. The Z-D calibration parameters for principal

distance c_i are the principal point offsets, $x_p^{(c_i)}$ and $y_p^{(c_i)}$, and $k_1^{(c_i)}$ the coefficient for the cubic radial lens distortion function.

The individual Z-D calibration parameters are obtained as follows:

1. Principal distance: $c_i = a_0 + a_1 f_i$
2. Principal point offsets: $x_p^{(c_i)} = b_0 + b_1 c_i$
3. Radial lens distortion: $k_1^{(c_i)} = d_0 + d_1 c_i^2$

CHAPTER SIX

RESULTS AND ANALYSIS

- 6.1 Introduction**
- 6.2 Used Software**
- 6.3 Used Hardware**
- 6.4 Camera Calibration**
- 6.5 Results**
- 6.6 Practical Examples**

6.1 Introduction

In this chapter, the results introduced of the field work. Mobile phone cameras are used to apply 3D models for close range objects. Several experiments on a 3D model were applied using set of mobile phones cameras from different manufactures and specifications.

6.2 Used Software

Different free software was used to make 3D models. These software are available online in internet to be freely downloaded. The software that were tested in this project are: Iinsight3D, Agisoft Stereoscan, 123D Catch, Meshlab and Agisoft Lenz.

6.2.1 Insight3d

Insight3d lets you create 3D models from a group of photographs. A series of photos of a real scene are used (e.g., of a building). It automatically matches them, then calculates positions in space from which each photo has been taken (plus camera's optical parameters) along with a 3D point cloud of the scene. Then insight3d's can be used as modeling tool to create textured polygonal model. It is a free open source application. Versions for both Linux and Windows operating systems are available on project's website. Figure (6-1) shows the main interface of the program. [15]

A series of photos to cover the whole scene you want to reconstruct. Several important rules should be remembered as recommended by the software developers:-

- The photos should be focused (not blurred).
- There should be large overlaps between neighboring photos up to 80%.
- There should be only limited angle difference between subsequent photos. When moving around an object. Photo should be every 15-25 degrees.
- Do not crop the images.

Insight3d can automatically determine all exterior orientation ($\omega, \phi, k, Xl, Yl, Zl$) parameters of the cameras used to acquire the photos (like their orientations in space or focal lengths) without having initial approximation matching about them. This is done in two steps:

- First the photos are matched. The application looks at each image, finds group of points in it Then tries to track these points on other photos using automatic matching techniques.
- The photos are then calibrated as discussed in chapter 5. This means that the positions of the camera and its other parameters including radial and tangential distortions when taking each picture are calculated from these tracked points. [15]

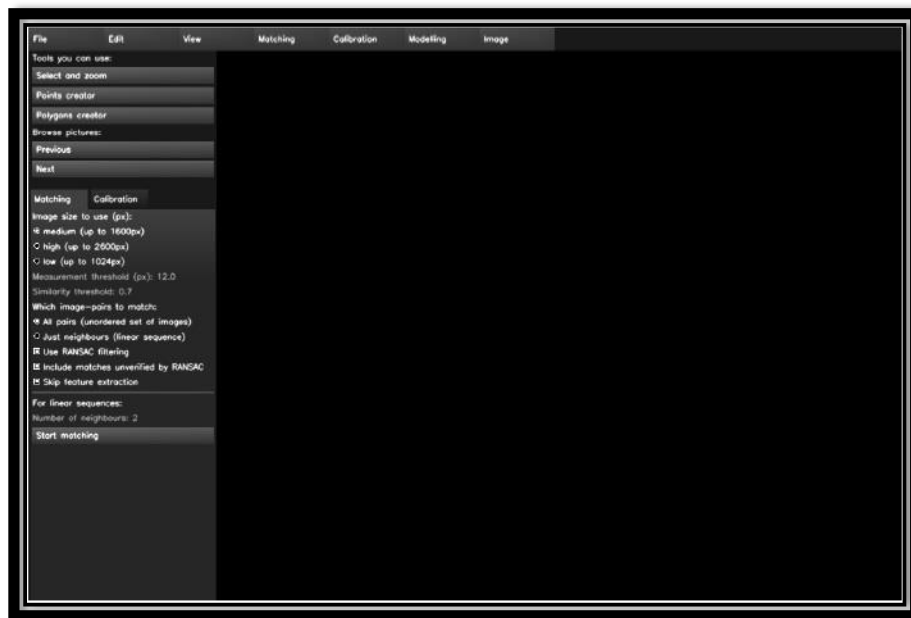


Figure (6 - 1) the main interface of Insight 3D

6.2.2 AgiSoft StereoScan

AgiSoft StereoScan is an easy to use 3D modeling tool for automatic generation of textured 3D models from individual stereopairs. The stereopairs are not required to be calibrated or aligned. The photos can be captured by hand from any generic positions.

Based on the photogrammetric, Stereoscan automatically calibrates the cameras, including camera positions and lens distortions. [16] As shown in figure (6-2).

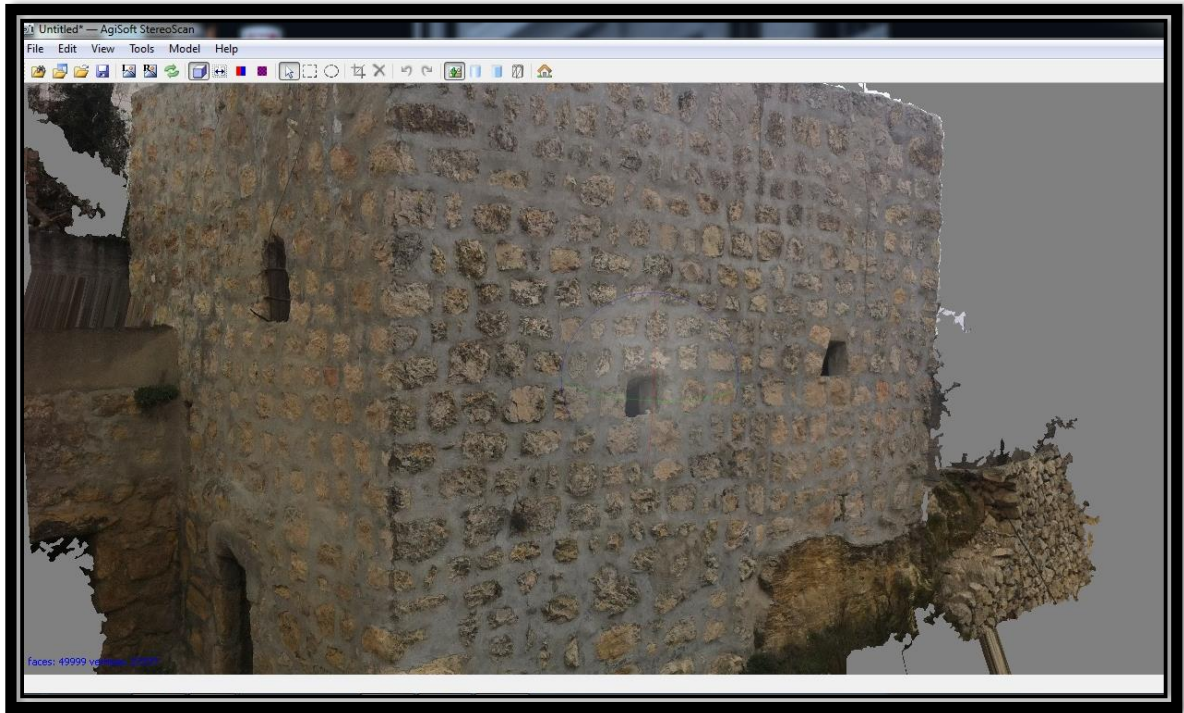


Figure (6 - 2) 3D model using Samsung Galaxy S4 in Agisoft StereoScan

6.2.3 123d catch

Autodesk 123D is a suite of hobbyist CAD and 3D modeling tools created by Autodesk. As well as the more basic drawing and modeling capabilities it also has assembly and constraint support of different export formats. Available for the software is also a library of ready-made blocks and objects as shown in figure (6-3).

Autodesk is also working in collaboration with three companies (Ponoko, Techshop and 3D Systems) to enable users of 123D to create physical objects from their designs using 3D printing technology. It is currently in freely downloadable with possibility of premium membership which enables more capabilities [17].

Cameras are used capture the people, places and things everywhere as amazingly realistic 3D experiences. Automatically, these are transformed into interactive 3D models

that can be shared with friends, family, and an ever growing community of 3D photographers.

- 3D models can be exported in a variety of formats from the 123D online community or in locally in the PC to be used by other software for use in other 3D tools and projects.

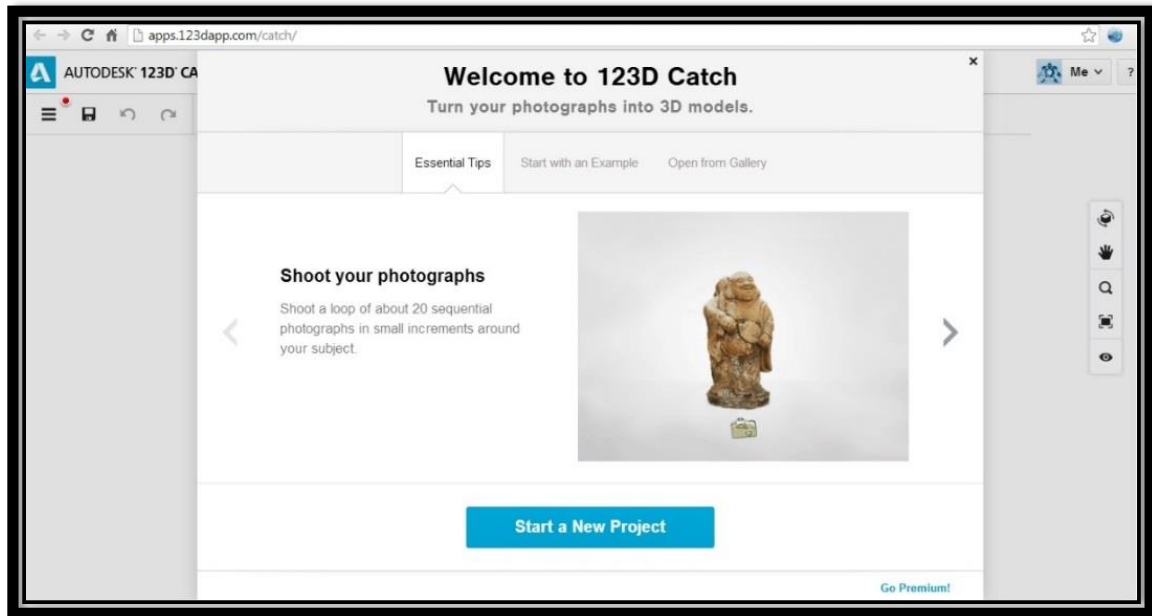


Figure (6 - 3) the main interface of 123D Catch.. [18]

6.2.4 Meshlab

An advanced 3D meshes processing software system, which is well known in the more technical fields of 3D development and data handling. Meshlab is a free and open-source software. Meshlab is subjected to the requirements of the GNU General Public License(GPL).

Meshlab is developed by the ISTI - CNR research center initially, Meshlab was created as a course assignment at the University of Pisa in late 2005. It is an open-source general-purpose system aimed at the processing of the typical not-so-small unstructured 3D models that arise in the 3D scanning pipeline [18]. See figure (6-4).

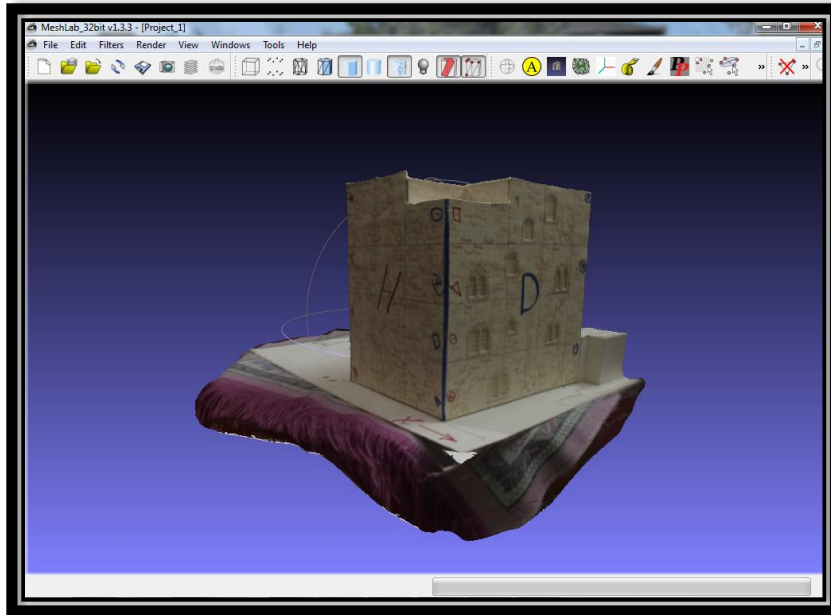


Figure (6 - 4) the main interface of meshlab

6.2.5 Agisoft Lenz

Figure (6-5) show us the main interface of Agisoft. Agisoft Lenz is automatic lens calibration software, which uses LCD screen as a calibration target. It supports estimation of the full camera calibration matrix, including non-linear distortion coefficients. Estimated calibration parameters can be saved in human readable file format for subsequent use in the software, where precise camera calibration data is required [19].

Agisoft Lenz estimates the following camera calibration parameters:

- f_x , f_y - focal length
- c_x , c_y - principal point coordinates
- K_1 , K_2 , K_3 , P_1 , P_2 - radial distortion coefficients, using Brown's distortion model

To capture photos of the calibration pattern:

1. Select Show chessboard command from the Tools menu to display the calibration pattern or press toolbar button, to open a window as shown in figure (6-6).

2. Capture a series of photos of the displayed calibration pattern with your camera from slightly different angles, according to the guidelines, outlined below. Minimum number of photos for a given focal length is 3.
3. If you are calibrating zoom lens, change the focal length of your lens and repeat step 2 for other focal length settings.
4. Click anywhere on the calibration pattern or press Escape button to return to the program.
5. Upload the captured photos to the computer.

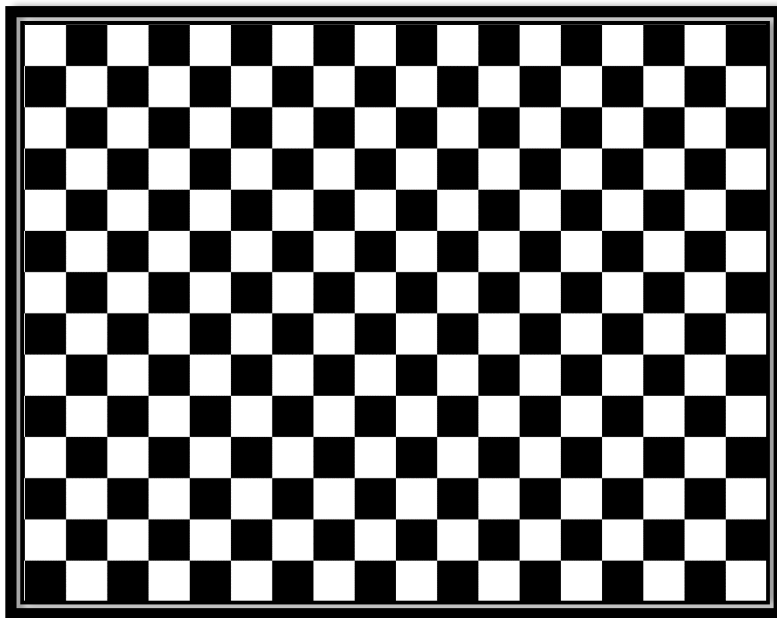


Figure (6 - 5) Chessboard

When capturing photos of the calibration pattern, try to fulfill the following guidelines:

- Make sure that the focal length keeps constant throughout the session (in case of zoom lens).
- Avoid glare on the photos. Move the light sources away if required.
- Preferably, the whole area of the photos should be covered by calibration pattern. Move the camera closer to the LCD screen if required.

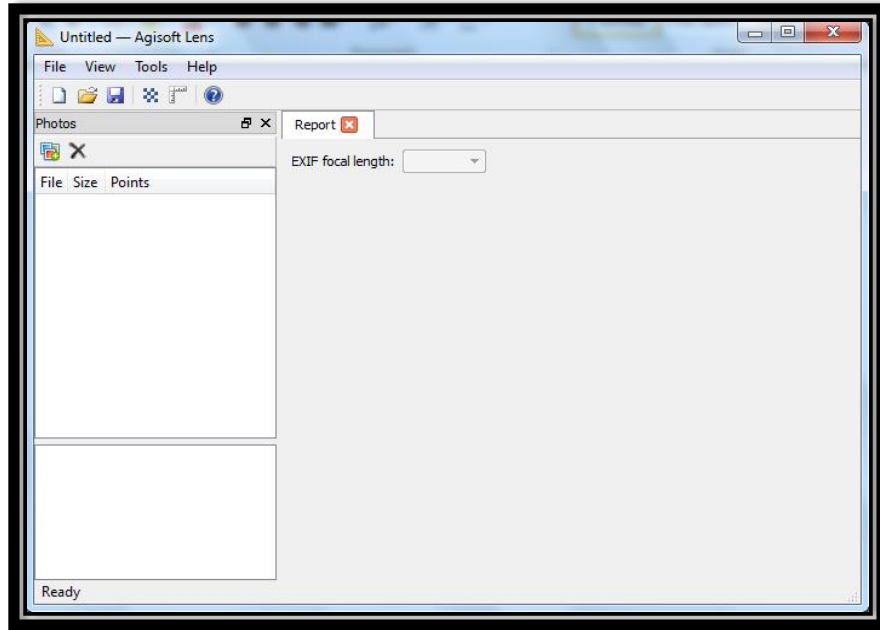


Figure (6 - 6) the main interface of Agisoft Lens

6.3 Used Hardware

Different mobile phones were used in order to make a comparison of different cameras with different specifications and resolutions. Nokia X3, I phone 4G, I phone 5S and Samsung Galaxy S4 were used in this project.

6.3.1 Nokia X3

As shown in table (6-1), the major properties of Nokia X3 phone are given. Figure (6-7) shows Nokia X3 mobile phone.

Table (6 - 1) Nokia X3 Properties . [20]

Phone Size	Dimensions	96 x 49.3 x 14.1 mm, 65.8 cc (3.78 x 1.94 x 0.56 in)
	Weight	103 grams
DISPLAY	Type	TFT, 256K colors
	Size	2.2 inches (~182 ppi pixel density)
	Resolution	240 x 320 pixels
DATA	GPRS	Class 32
	EDGE	Class 32, 296 / 178.8 kbits
	Bluetooth	Yes, v2.1 with A2DP
CAMERA	Primary	3.2 MP, 2048 x 1536 pixels, enhanced fixed focus
	Video	Yes, QCIF@15fps
	Secondary	No



Figure (6 - 7) Nokia X3

6.3.2 I phone 4G

As shown in table (6-2), the major properties of I phone 4G phone are given. Figure (6-8) shows I phone 4G mobile phone.

Table (6 - 2) I phone 4G Properties . [21]

Phone Size	Dimensions	115.2 x 58.6 x 9.3 mm
	Weight	135 grams
DISPLAY	Type	LED-backlit IPS TFT, 16M colors
	Size	3.5 inches
	Resolution	640 x 960 pixels
CAMERA	Primary	5 MP, 2592 x 1944 pixels
	Video	HD, 720p@30fps
	Features	LED flash, Autofocus, Geo-tagging, touch focus, LED video light
	Secondary	VGA, Video calling over Wi-Fi only
Software	OS	ios 4
	Processor	1 GHz ARM Cortex-A8 processor, PowerVR SGX535GPU, Apple A4 chipset
	RAM	512 MB RAM



Figure (6 - 8) I phone 4G

6.3.3 I phone 5S

As shown in table (6-3), the major properties of I phone 5S phone are given. Figure (6-9) shows I phone 5S mobile phone.

Table (6 - 3) I phone 5S Properties. [22]

Phone Size	Dimensions	123.8 x 58.6 x 7.6 mm (4.87 x 2.31 x 0.30 in)
	Weight	112 grams
DISPLAY	Type	LED-backlit IPS LCD, capacitive touchscreen, 16M colors
	Size	4.0 inches (~326 ppi pixel density)
	Resolution	640 x 1136 pixels
CAMERA	Primary	8 MP, 3264 x 2448 pixels, autofocus, dual-LED (dual tone) flash
	Video	Yes, 1080p@30fps, 720p@120fps, video stabilization
	Features	1/3" sensor size, 1.5 µm pixel size, simultaneous HD video and image recording, touch focus, geo-tagging, face detection, HDR panorama, HDR photo
	Secondary	Yes, 1.2 MP, 720p@30fps, face detection, FaceTime over Wi-Fi or Cellular
FEATURES	OS	iOS 7, upgradable to iOS 7.1
	CPU	Dual-core 1.3 GHz Cyclone (ARM v8-based)
	GPU	PowerVR G6430 (quad-core graphics)



Figure (6 - 9) I phone 5S

6.4 Camera Calibration

As described in chapter 5 about camera calibration. The calibration elements were found in this project automatically by using Agisoft Lenz. The parameters that were calculated for each mobile phone camera are shown in figures (6-10), (6-11) and (6-12). The principle of it described in chapter (6.2.5). Agisoft Lenz estimates the following camera calibration parameters:

- f_x , f_y - focal length
- c_x , c_y - principal point coordinates
- K_1 , K_2 , K_3 , P_1 , P_2 - radial distortion coefficients, using Brown's distortion model

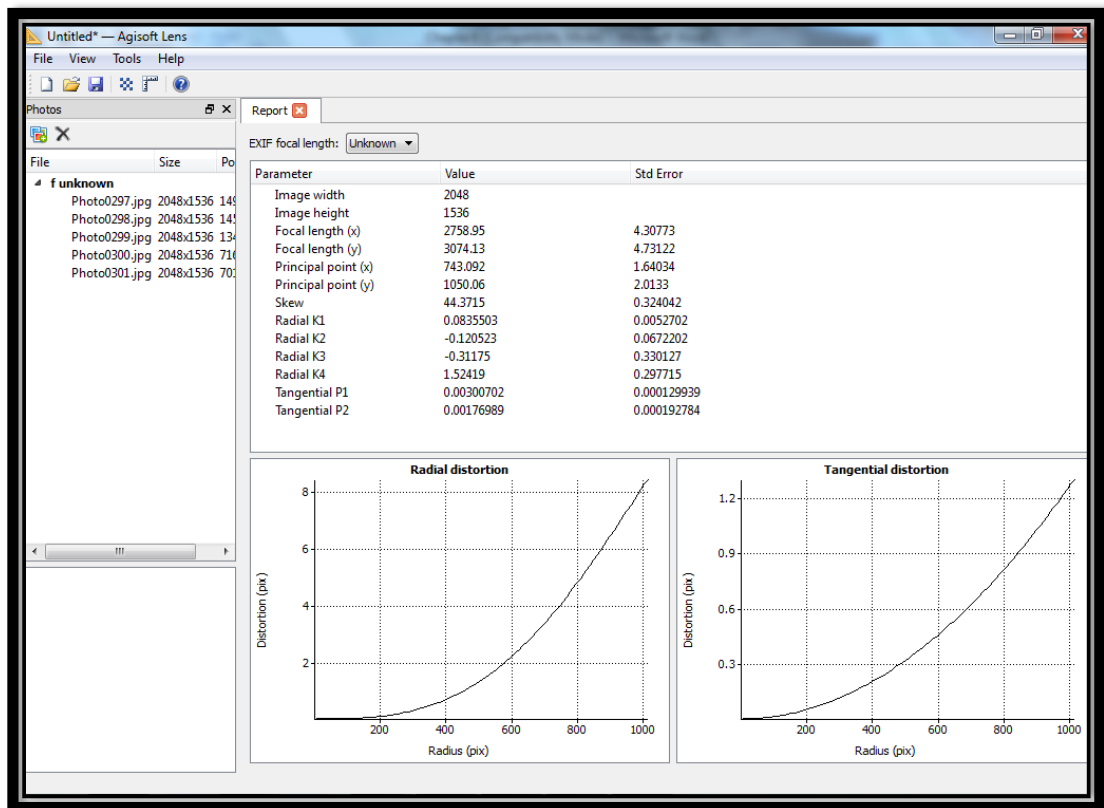


Figure (6 - 10) Camera Calibration for Nokia X3 mobile phone

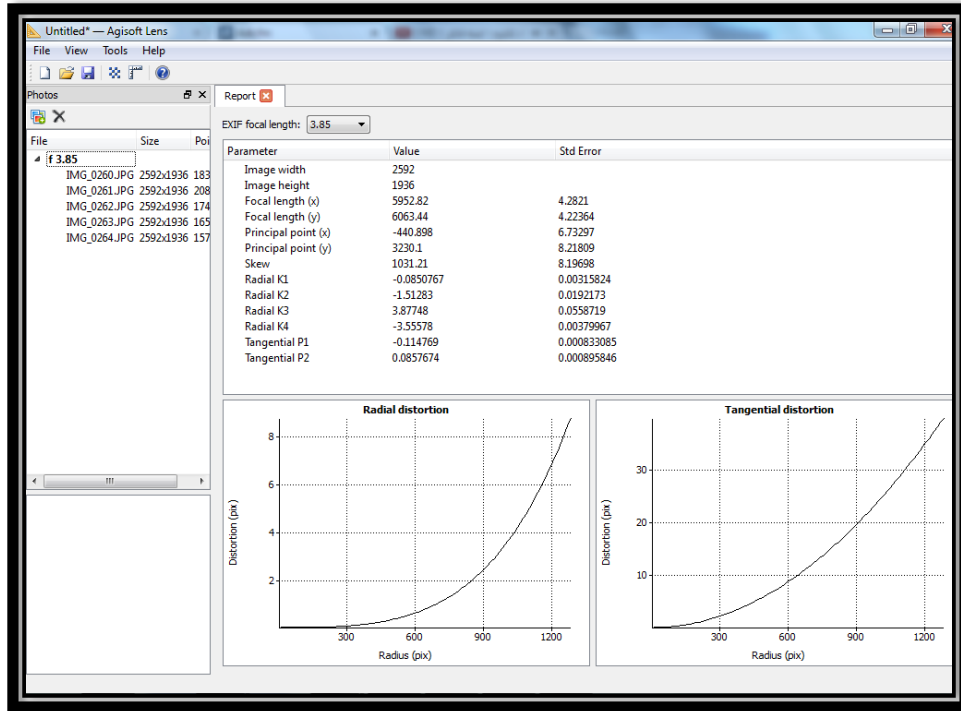


Figure (6 - 11) Camera Calibration for I phone 4G mobile phone

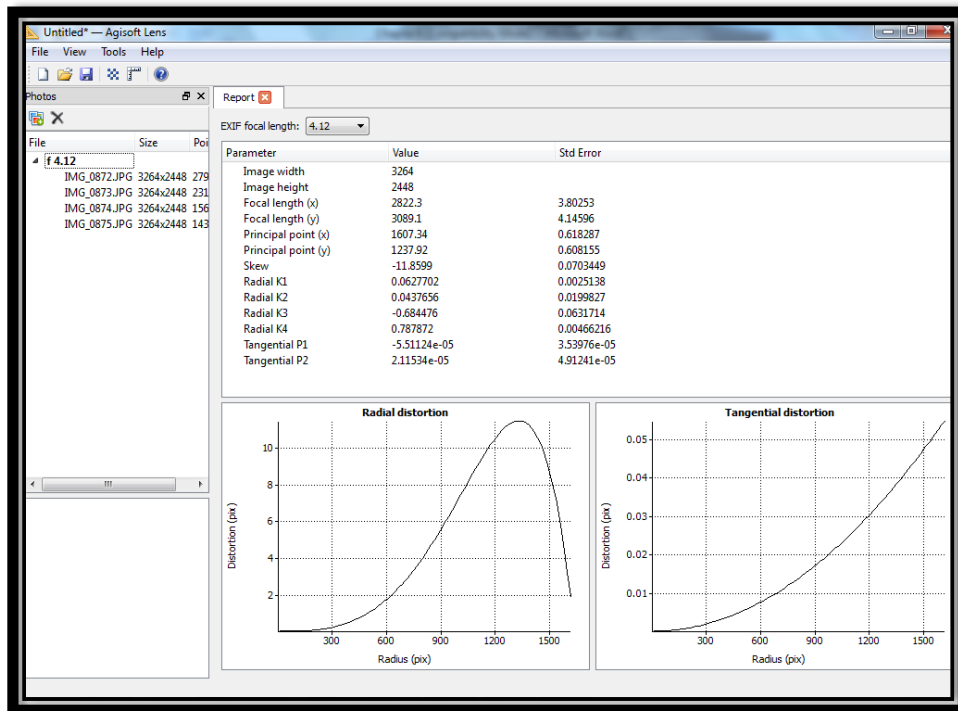


Figure (6 - 12) Camera Calibration for I phone 5S mobile phone

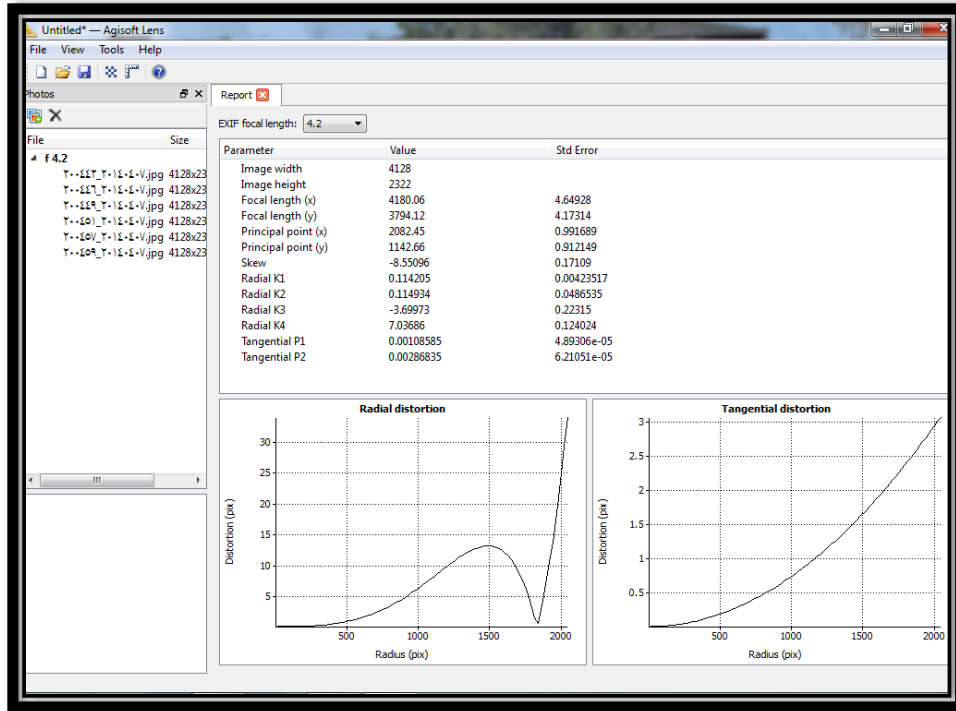


Figure (6 - 13) Camera Calibration for Samsung Galaxy S4 mobile phone

6.5 Results

Four different models were used for testing in this project, in order to make a comparison with different mobile phone with different cameras resolution, as described in chapter (6.3). The models and their results are described in the following sections. The reference distance were measured in the real objects using a caliber with accuracy of ± 0.05 mm, the same point are measured on the 3D model on meshlab software.

6.5.1 Model #1

A 3D model can build by the students of Architectural engineering at the Palestine Polytechnic University. This model consists of a two-story residential building as shown in figure (6-14). The results of the modeling of this object are discussed in the chapter (6.5.1.1-6.5.1.3).



Figure (6 - 14) Model #1

6.5.1.1 Nokia X3

After capturing pictures of model #1 from all sides by Nokia X3 phone, 123D catch software was used to make a 3D model. The model was opened using Meshlab software in order to make a required measurement on the model as shown in figure (6-15). The results show the comparison between the real distances and the same distances measured in the 3D model created using Nokia X3 phone photos, as shown in table (6-4).

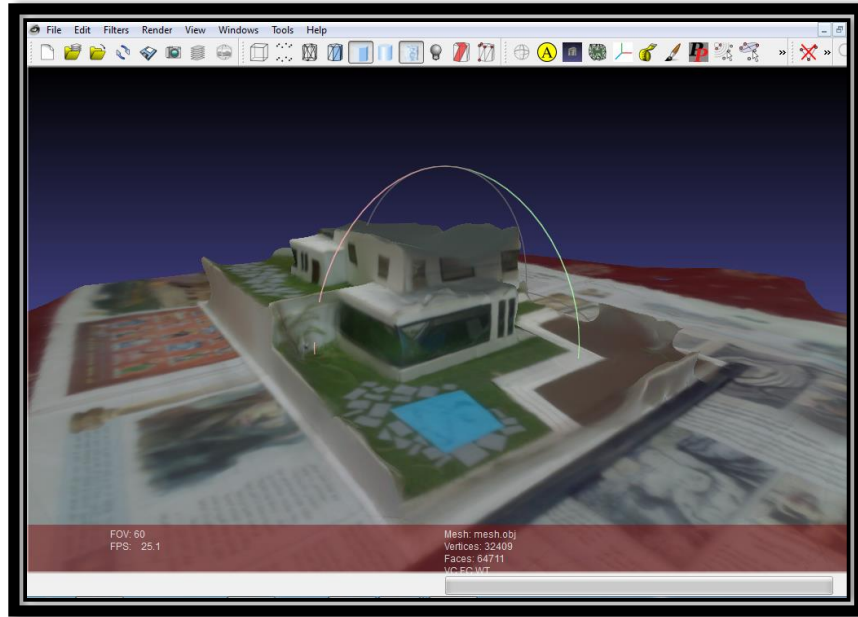


Figure (6 - 15) Model #1 by Nokia X3 in Meshlab

Table (6 - 4) Model #1 by Nokia X3 results

#	Model distance (mm)	Program distance (mm)	Δd
1	7.00	7.19779	+0.19779
2	8.00	7.85105	-0.14895
3	12.0	11.7247	-0.27530
4	18.0	18.2183	+0.21830
5	19.0	19.2533	+0.25330
6	24.0	23.4813	-0.48130
7	27.0	27.3287	+0.32870
8	31.0	30.7581	-0.24190
9	51.0	51.2126	+0.21260
10	70.0	70.1912	+0.19120

Min= 0.14895

Max= 0.48130

Avg=0.25493

Standard errors and errors of other percent probabilities are commonly used to evaluate measurements for acceptance against blunders and mistakes. Project specifications and contracts often require that acceptable errors be within specified limits, such as the 95% and 99.9% and 95% errors.

So $E_{95} = 1.960\sigma$

$$E_{99.9} = 3.290\sigma$$

$$E_{95} = 1.960 * 0.25493 = 0.49966$$

$$E_{99.9} = 3.290 * 0.25493 = 0.83872$$

At 95% level of confidence, test measurements are accepted against blunders. Finally, the root mean square error RMSE is used to represent the accuracy.

$$RMSE = \sqrt{\frac{\sum X^2}{n}} = 0.26998$$

6.5.1.2 I phone 4G

After capturing pictures of model #1 from all sides by I phone 4G phone, 123D catch software was used to make a 3D model. The model was opened using Meshlab software in order to make a required measurement on the model as shown in figure (6-16). The results show the comparison between the real distances and the same distances measured in the 3D model created using I phone 4G phone photos, as shown in table (6-5).

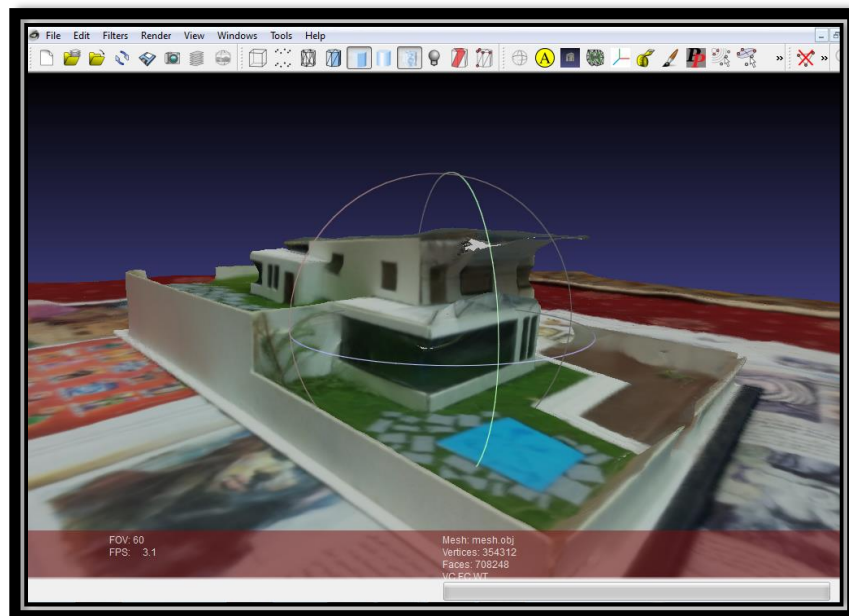


Figure (6 - 16) Model #1 by I phone 4G in Meshlab

Table (6 - 5) Model #1 by I phone 4G results

#	Model distance (mm)	Program distance (mm)	Δd
1	7.00	7.10047	+0.10047
2	8.00	7.85105	-0.10620
3	12.0	12.0911	+0.09110
4	18.0	18.1102	+0.11020
5	19.0	19.1433	+0.14330
6	24.0	23.8813	-0.11870
7	27.0	27.1287	+0.12870
8	31.0	30.8581	-0.14190
9	51.0	51.0126	+0.01260
10	70.0	70.1012	+0.10120

Min= 0.01260

Max= 0.14330

Avg=0.10544

$E_{95} = 1.960 * 0.10544 = 0.20666$

At 95% level of confidence the observations were accepted against blunders. Finally the RMSE was = 0.11115

6.5.1.3 I phone 5S

After capturing pictures of model #1 from all sides by I phone 5S phone, 123D catch software was used to make a 3D model. The model is opened using Meshlab software in order to make a required measurement on the model as shown in figure (6-17). The results show the comparison between the real distances and the same distances measured in the 3D model created using I phone 5S phone photos, as shown in table (6-6).

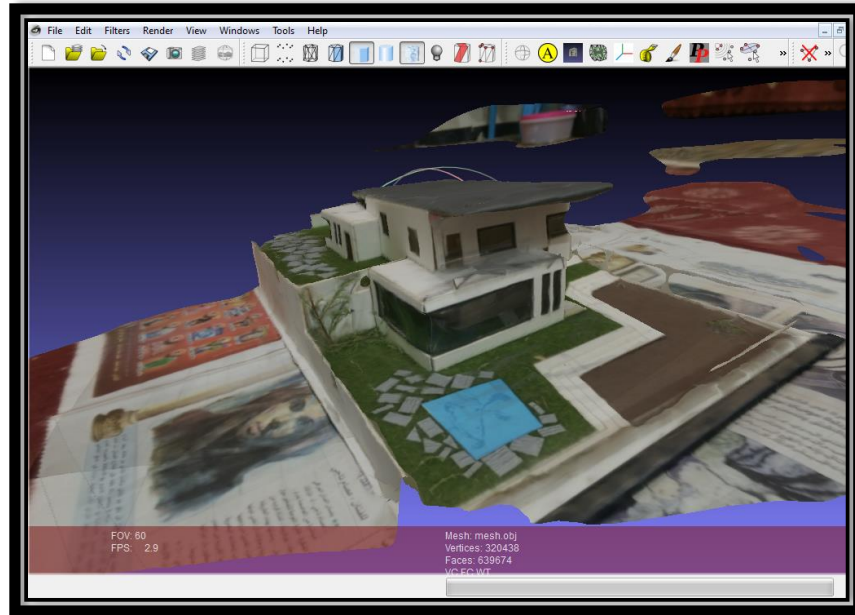


Figure (6 - 17) Model #1 by I phone 5S in Meshlab

Table (6 - 6) Model #1 by I phone 5S results

#	Model distance (mm)	Program distance (mm)	Δ d
1	7.00	7.00450	+0.00450
2	8.00	7.90770	-0.09230
3	12.0	11.99240	-0.00760
4	18.0	18.02390	+0.02390
5	19.0	19.05130	+0.05130
6	24.0	23.91840	-0.08160
7	27.0	27.01570	+0.01570
8	31.0	30.93790	-0.06210
9	51.0	51.03760	+0.03760
10	70.0	70.08120	+0.08120

Min= 0.00450

Max= 0.09230

Avg=0.04578

$$E_{95} = 1.960 * 0.04578 = 0.08972$$

At 95% level of confidence the observations were accepted against blunders. Finally the RMSE was = 0.055289

6.5.2 Model #2

A 3D model can build by the students of Architectural engineering at the Palestine Polytechnic University. This model is a church west of design, as shown in figure (6-18). The results of the modeling of this object are discussed in the chapter (6.5.2.1-6.5.2.3).

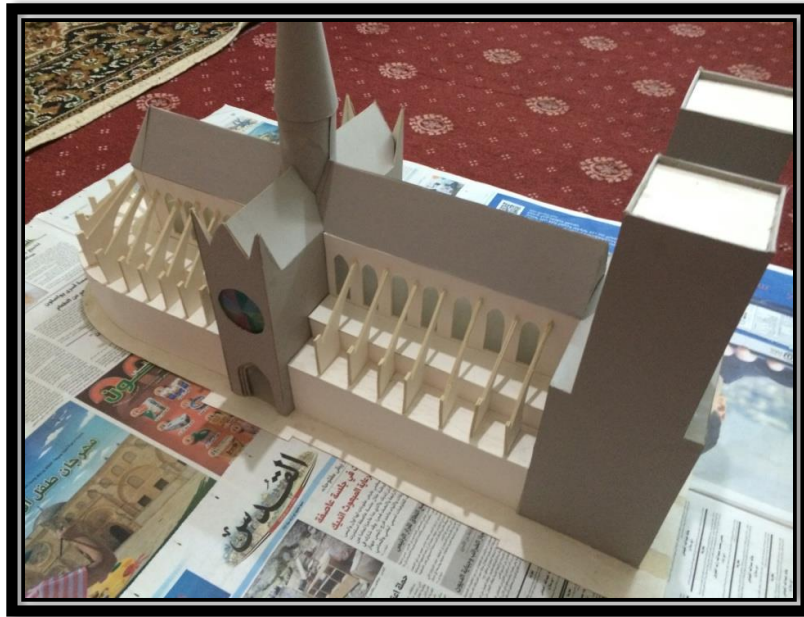


Figure (6 - 18) Model #2

6.5.2.1 Nokia X3

After capturing pictures of model #2 from all sides by Nokia X3 phone, 123D catch software was used to make a 3D model. The model is opened using Meshlab software in order to make a required measurement on the model as shown in figure (6-19). The results show the comparison between the real distances and the same distances measured in the 3D model created using Nokia X3 phone photos, as shown in table (6-7).

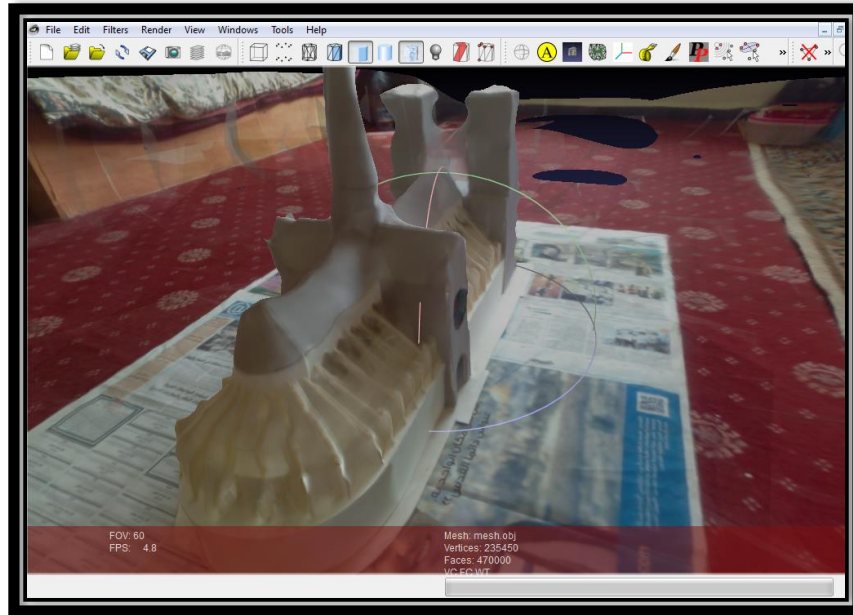


Figure (6 - 19) Model #2 by Nokia X3 in Meshlab

Table (6 - 7) Model #2 by Nokia X3 results

#	Model distance (mm)	Program distance (mm)	Δd
1	7.00	7.19001	+0.19001
2	8.00	7.65890	-0.34110
3	12.0	11.71580	-0.28420
4	17.0	17.49310	+0.49310
5	18.0	18.40110	+0.40110
6	20.0	19.74670	-0.25330
7	25.5	25.19040	-0.30960
8	30.0	30.14130	+0.14130
9	40.0	40.23360	+0.23360
10	45.0	45.17710	+0.17710

Min= 0.147710

Max= 0.49310

Avg=0.28244

$E_{95} = 1.960 * 0.28244 = 0.55358$

At 95% level of confidence the observations were accepted against blunders. Finally the RMSE was = 0.300527

6.5.2.2 I phone 4G

After capturing pictures of model #2 from all sides by I phone 4G phone, 123D catch software was used to make a 3D model. The model is opened using Meshlab software in order to make a required measurement on the model as shown in figure (6-20). The results show the comparison between the real distances and the same distances measured in the 3D model created using I phone 4G phone photos, as shown in table (6-8).

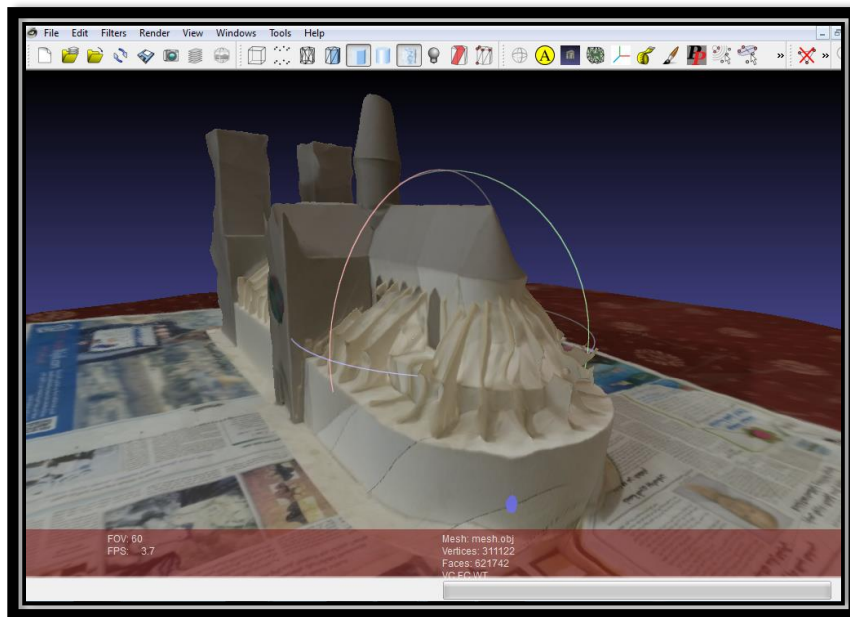


Figure (6 - 20) Model #2 by I phone 4G in Meshlab

Table (6 - 8) Model #2 by I phone 4G results

#	Model distance (mm)	Program distance (mm)	Δd
1	7.00	7.10021	+0.10021
2	8.00	7.85870	-0.14130
3	12.0	11.88670	-0.11330
4	17.0	17.09032	+0.09032
5	18.0	18.12730	+0.12730
6	20.0	19.89550	-0.10450
7	25.5	25.39130	-0.10870
8	30.0	30.14010	+0.14010
9	40.0	40.13220	+0.13220
10	45.0	45.10710	+0.10710

Min= 0.09032

Max= 0.14130

Avg=0.11650

$E_{95} = 1.960 * 0.11650 = 0.22834$

At 95% level of confidence the observations were accepted against blunders. Finally the RMSE was = 0.11769

6.5.2.3 I phone 5S

After capturing pictures of model #2 from all sides by I phone 5S phone, 123D catch software was used to make a 3D model. The model is opened using Meshlab software in order to make a required measurement on the model as shown in figure (6-21). The results show the comparison between the real distances and the same distances measured in the 3D model created using I phone 5S phone photos, as shown in table (6-9).

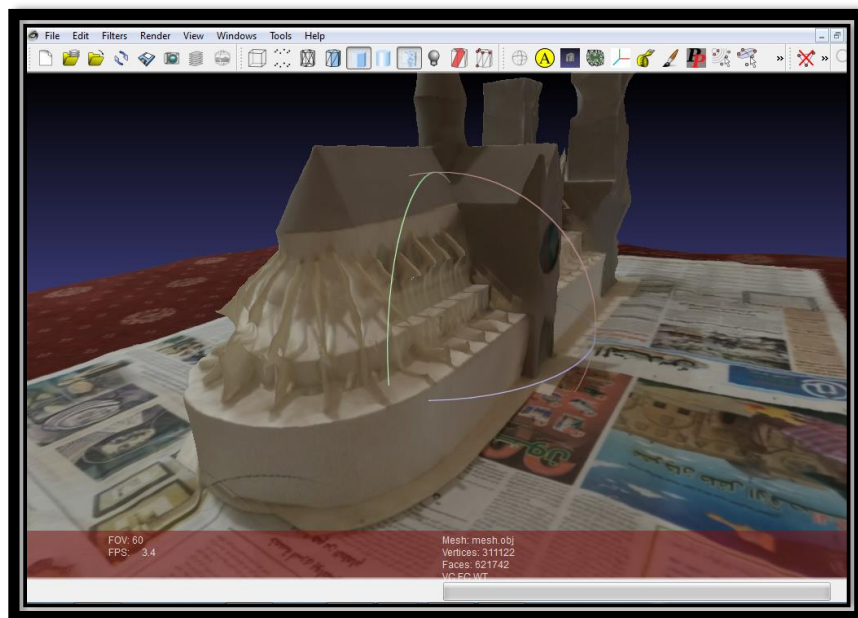


Figure (6 - 21) Model #2 by I phone 5S in Meshlab

Table (6 - 9) Model #2 by I phone 5S results

#	Model distance (mm)	Program distance (mm)	Δd
1	7.00	7.00770	+0.00770
2	8.00	7.96650	-0.03350
3	12.0	11.99090	-0.00910
4	17.0	17.02410	+0.02410
5	18.0	18.08330	+0.08330
6	20.0	19.93480	-0.06520
7	25.5	25.48340	-0.01660
8	30.0	29.92490	-0.07510
9	40.0	40.04720	+0.04720
10	45.0	45.01800	+0.01800

Min= 0.00770

Max= 0.08330

Avg=0.03798

$E_{95} = 1.960 * 0.03798 = 0.07444$

At 95% level of confidence the observations were accepted against blunders. Finally the RMSE was = 0.046371

6.5.3 Model #3

A 3D model can build by the students of Architectural engineering at the Palestine Polytechnic University so that model is a residential building as shown in figure (6-22). The results of the modeling of this object are discussed in the chapter (6.5.3.1-6.5.3.3).



Figure (6 - 22) Model #3

6.5.3.1 Nokia X3

After capturing pictures of model #3 from all sides by Nokia X3 phone, 123D catch software was used to make a 3D model. The model is opened using Meshlab software in order to make a required measurement on the model as shown in figure (6-23). The results show the comparison between the real distances and the same distances measured in the 3D model created using Nokia X3 phone photos, as shown in table (6-10).

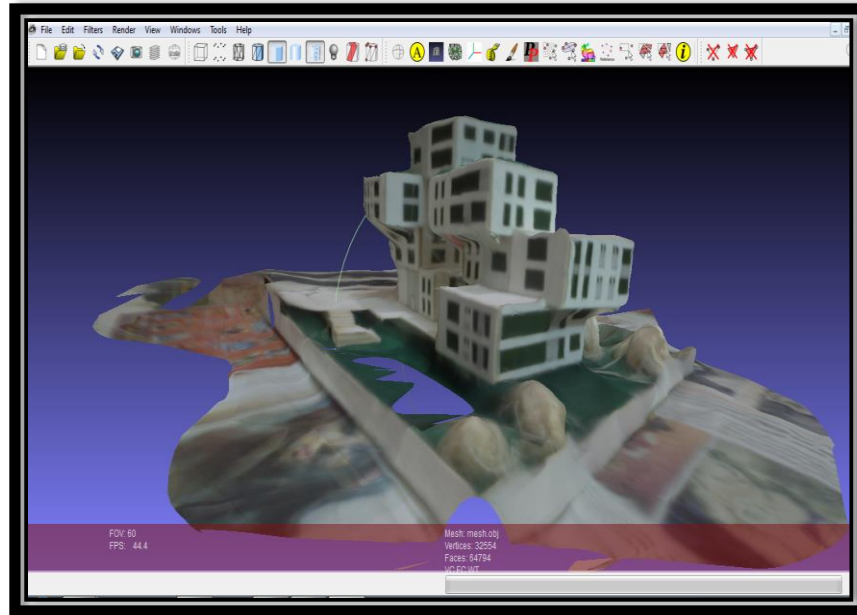


Figure (6 - 23) Model #3 by Nokia X3 in Meshlab

Table (6 - 10) Model #3 by Nokia X3 results

#	Model distance (mm)	Program distance (mm)	Δd
1	5.00	5.43160	+0.43160
2	9.00	8.70770	-0.29230
3	10.0	10.36240	+0.36240
4	14.0	13.69610	-0.30390
5	17.0	17.40130	+0.40130
6	18.0	18.28740	+0.28740
7	20.0	19.64280	-0.35720
8	35.0	35.27910	+0.27910
9	61.0	61.44160	+0.44160
10	74.0	74.30120	+0.30120

Min= 0.27910

Max= 0.44160

Avg=0.34580

$E_{95} = 1.960 * 0.34580 = 0.67777$

At 95% level of confidence the observations were accepted against blunders. Finally the RMSE was = 0.35075

6.5.3.2 I phone 4G

After capturing pictures of model #3 from all sides by I phone 4G phone, 123D catch software was used to make a 3D model. The model is opened using Meshlab software in order to make a required measurement on the model as shown in figure (6-24). The results show the comparison between the real distances and the same distances measured in the 3D model created using I phone 4G phone photos, as shown in table (6-11).

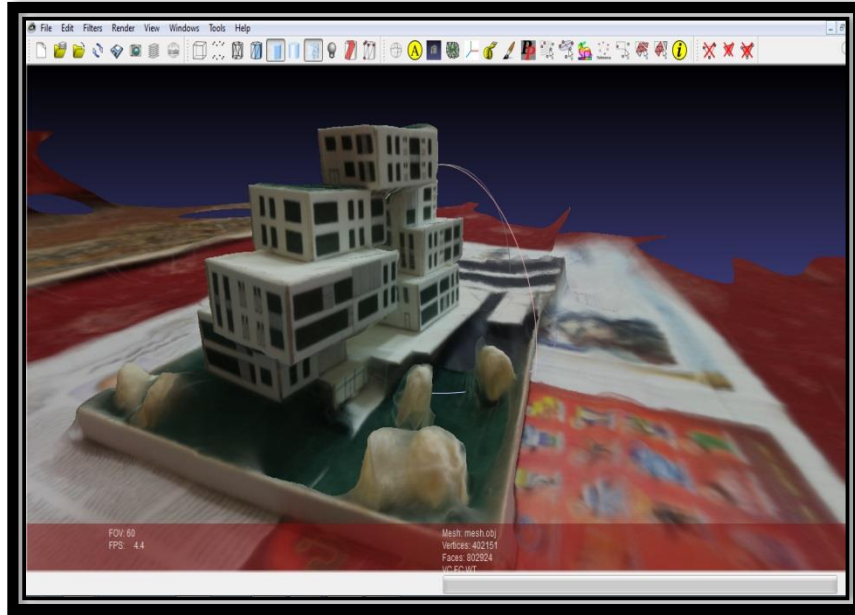


Figure (6 - 24) Model #3 by I phone 4G in Meshlab

Table (6 - 11) Model #3 by I phone 4G results

#	Model distance (mm)	Program distance (mm)	Δd
1	5.00	5.11460	+0.11460
2	9.00	8.86370	-0.13630
3	10.0	10.08240	+0.08240
4	14.0	13.85610	-0.14390
5	17.0	17.10170	+0.10170
6	18.0	18.12440	+0.12440
7	20.0	19.89280	-0.10720
8	35.0	35.10330	+0.10330
9	61.0	61.09460	+0.09460
10	74.0	74.08120	+0.08920

Min= 0.08240

Max= 0.14390

Avg=0.10976

$E_{95} = 1.960 * 0.10976 = 0.21513$

At 95% level of confidence the observations were accepted against blunders. Finally the RMSE was = 0.111398

6.5.3.3 I phone 5S

After capturing pictures of model #3 from all sides by I phone 5S phone, 123D catch software was used to make a 3D model. The model is opened using Meshlab software in order to make a required measurement on the model as shown in figure (6-25). The results show the comparison between the real distances and the same distances measured in the 3D model created using I phone 5S phone photos, as shown in table (6-12).

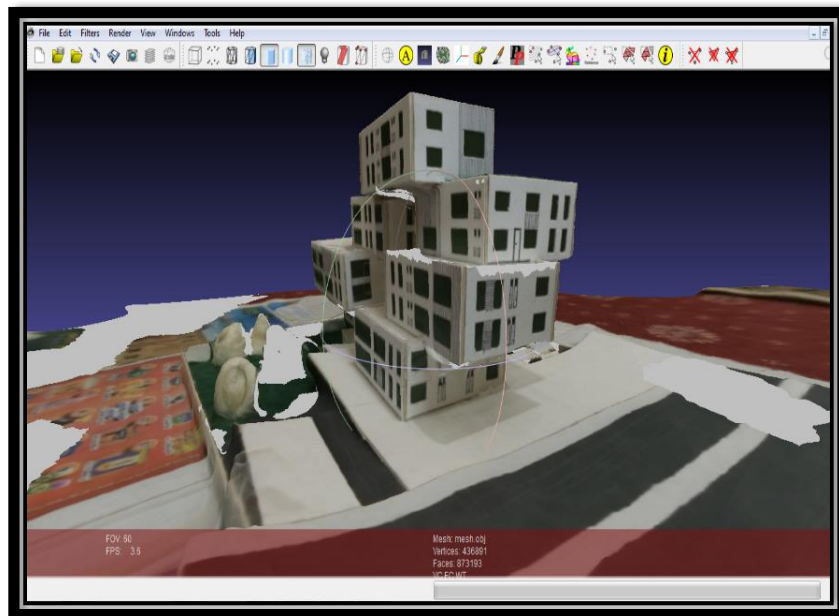


Figure (6 - 25) Model #3 by I phone 5S in Meshlab

Table (6 - 12) Model #3 by I phone 5S results

#	Model distance (mm)	Program distance (mm)	Δd
1	5.00	5.04260	+0.04260
2	9.00	8.91860	-0.08140
3	10.0	10.01240	+0.01240
4	14.0	13.94610	-0.05390
5	17.0	17.00540	+0.00540
6	18.0	18.07340	+0.07340
7	20.0	19.99580	-0.00420
8	35.0	35.06530	+0.06530
9	61.0	61.09110	+0.09110
10	74.0	74.03810	+0.03810

Min= 0.00420

Max= 0.09110

Avg=0.04678

 $E_{95} = 1.960 * 0.04678 = 0.09169$

At 95% level of confidence the observations were accepted against blunders. Finally the RMSE was = 0.055632

6.5.4 Model #4

A 3D model can build by the students of architectural at the Palestine Polytechnic University so that model is a cultural center as shown in figure (6-26). The results of the modeling of this object are discussed in the chapter (6.5.4.1-6.5.4.3).



Figure (6 - 26) Model #4

6.5.4.1 Nokia X3

After capturing pictures of model #4 from all sides by Nokia X3 phone, 123D catch software was used to make a 3D model. The model is opened using Meshlab software in order to make a required measurement on the model as shown in figure (6-27). The results show the comparison between the real distances and the same distances measured in the 3D model created using Nokia X3 phone photos, as shown in table (6-13).

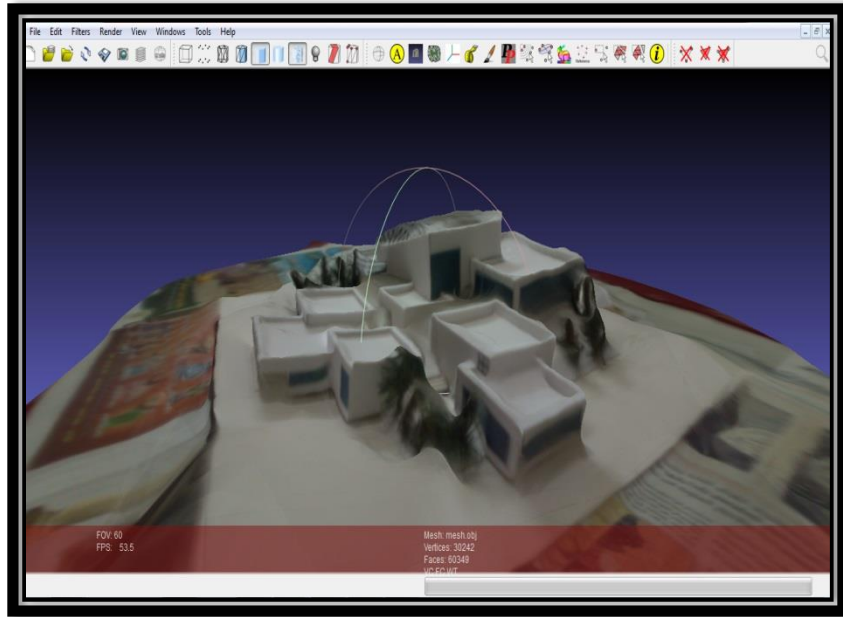


Figure (6 - 27) Model #4 by Nokia X3 in Meshlab

Table (6 - 13) Model #4 by Nokia X3 results

#	Model distance (mm)	Program distance (mm)	Δ d
1	4.00	4.42160	+0.42160
2	12.00	11.78360	-0.21640
3	15.0	15.27220	+0.27220
4	18.0	18.19390	+0.19390
5	19.0	18.64160	-0.35840
6	22.0	22.27450	+0.27450
7	32.0	31.57420	-0.42580
8	48.0	48.30530	+0.30530
9	50.0	49.79940	-0.20060
10	52.0	52.41040	+0.41040

Min= 0.19390

Max= 0.42580

Avg=0.30791

$E_{95} = 1.960 * 0.30791 = 0.60350$

At 95% level of confidence the observations were accepted against blunders. Finally the RMSE was = 0.31988

6.5.4.2 I phone 4G

After capturing pictures of model #4 from all sides by I phone 4G phone, 123D catch software was used to make a 3D model. The model is opened using Meshlab software in order to make a required measurement on the model as shown in figure (6-28). The results show the comparison between the real distances and the same distances measured in the 3D model created using I phone 4G phone photos, as shown in table (6-14).

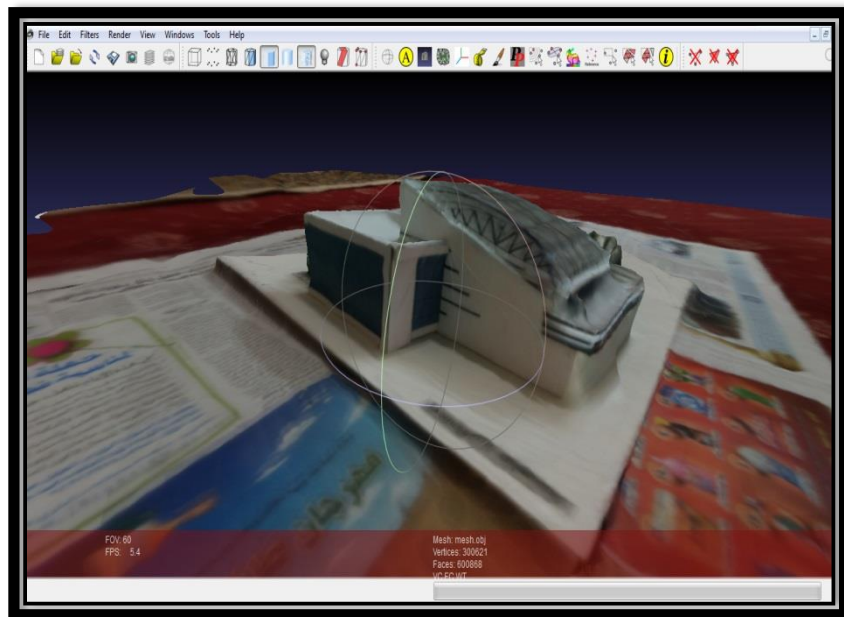


Figure (6 - 28) Model #4 by I phone 4G in Meshlab

Table (6 - 14) Model #4 by I phone 4G results

#	Model distance (mm)	Program distance (mm)	Δd
1	4.00	4.09320	+0.09320
2	12.00	11.86280	-0.13720
3	15.0	15.10110	+0.10110
4	18.0	18.08820	+0.08820
5	19.0	18.85160	-0.14840
6	22.0	22.10060	+0.10060
7	32.0	31.90850	-0.09150
8	48.0	48.12380	+0.12380
9	50.0	49.85940	-0.14060
10	52.0	52.15330	+0.15330

Min= 0.08820

Max= 0.15330

Avg=0.11779

$E_{95} = 1.960 * 0.11779 = 0.23087$

At 95% level of confidence the observations were accepted against blunders. Finally the RMSE was = 0.120526

6.5.4.3 I phone 5S

After capturing pictures of model #4 from all sides by I phone 5S phone, 123D catch software was used to make a 3D model. The model is opened using Meshlab software in order to make a required measurement on the model as shown in figure (6-29). The results show the comparison between the real distances and the same distances measured in the 3D model created using I phone 5S phone photos, as shown in table (6-15).

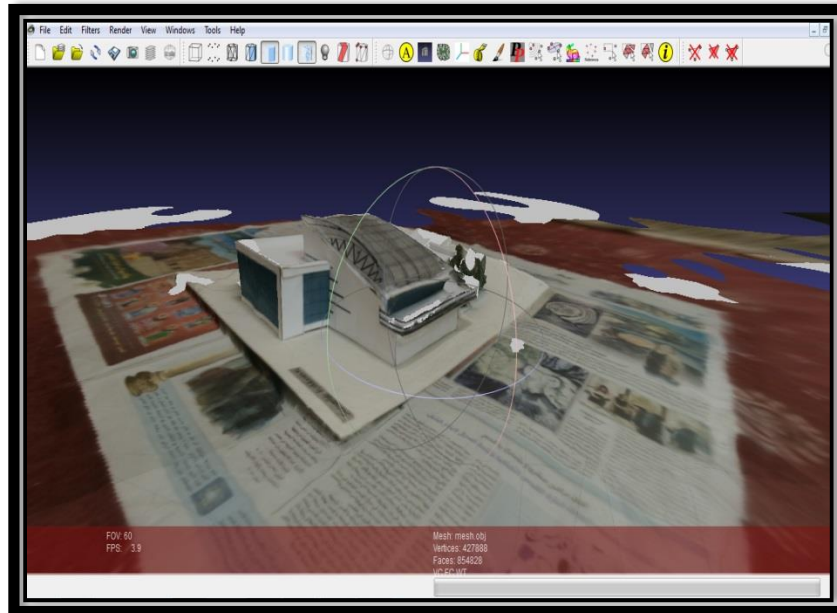


Figure (6 - 29) Model #4 by I phone 5S in Meshlab

Table (6 - 15) Model #4 by I phone 5S results

#	Model distance (mm)	Program distance (mm)	Δd
1	4.00	4.00950	+0.00950
2	12.00	11.95690	-0.04310
3	15.0	15.01610	+0.01610
4	18.0	18.05620	+0.05620
5	19.0	18.96190	-0.03810
6	22.0	22.01060	+0.01060
7	32.0	31.04210	-0.04210
8	48.0	48.02820	+0.02820
9	50.0	49.99160	-0.00840
10	52.0	52.04830	+0.04830

Min= 0.00840

Max= 0.09080

Avg=0.03006

 $E_{95} = 1.960 * 0.03493 = 0.06846$

At 95% level of confidence the observations were accepted against blunders. Finally the RMSE was = 0.034497

6.6 Practical examples

After the creation of the necessary calculations and measurements, the Ibrahimi Mosque and old building and were captured and used of three-dimensional modeling, as practical application of 3D modeling using mobile phones.

6.6.1 Old building

A group of pictures of an old building were captured different sides as shown in figure (6-30). 123D catch was used to make a 3D model. The model opened using Meshlab as shown in figure (6-31). Here it can be scaled and viewed from all sides, and measurements can be applied to archeology and documentation applications.



Figure (6 - 30) Old building

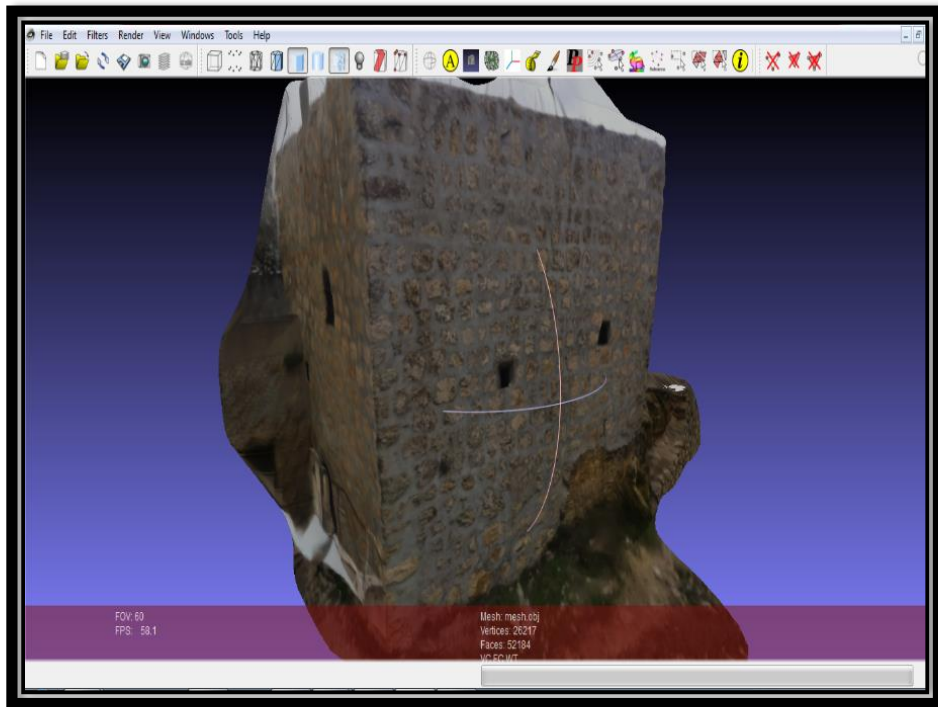


Figure (6 - 31) Old building in Meshlab

6.6.2 Ibrahimi Mosque

After we capture a lot of pictures in Ibrahimi mosque as shown in figure (6-32) and figure (6-33) and use 123D catch to make a 3D models, we install models and use Meshlab as shown in figure (6-34) and figure (6-35).

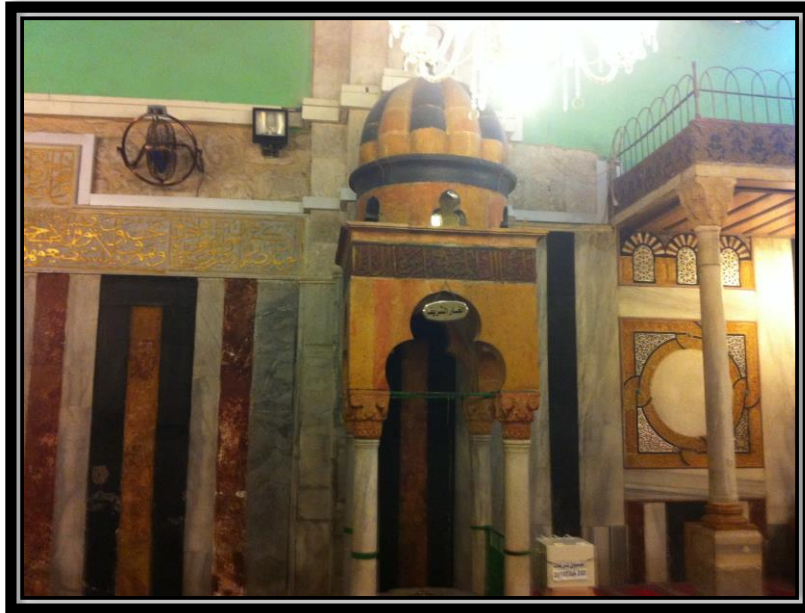


Figure (6 - 32) Alqhar Alshareef

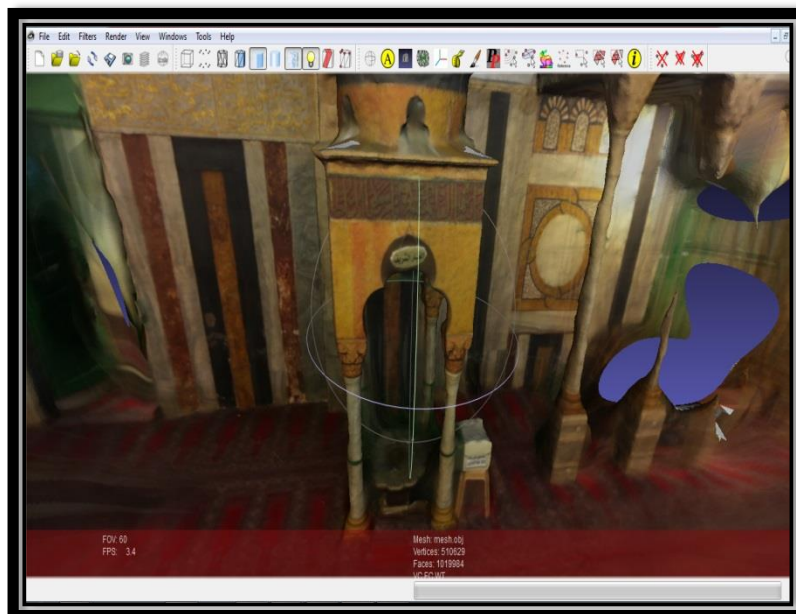


Figure (6 - 33) Alqhar Alshareef in Meshlab

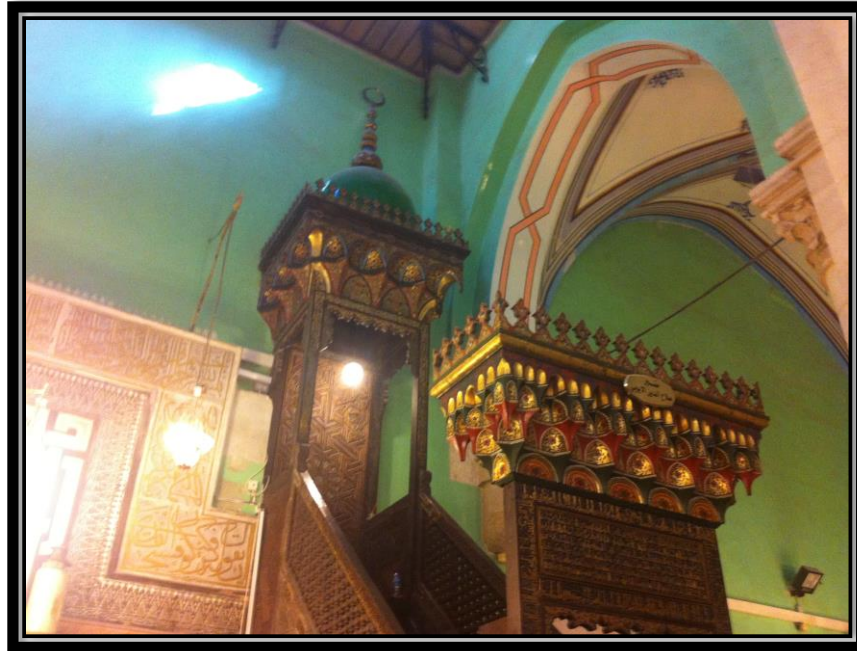


Figure (6 - 34) Menbar Salah Aldeen

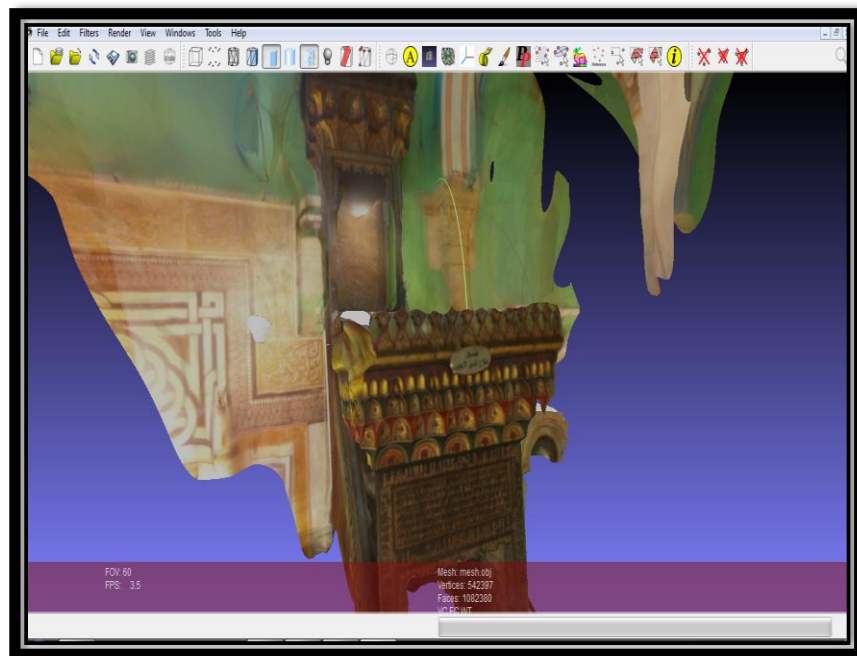


Figure (6 - 35) Menbar Salah Aldeen in Meshlab

6.6.3 Cemetery

As shown in figure (6-36) a cemetery as a photo and in figure (6-37) as a 3D Model.



Figure (6 - 36) Cemetery as photo

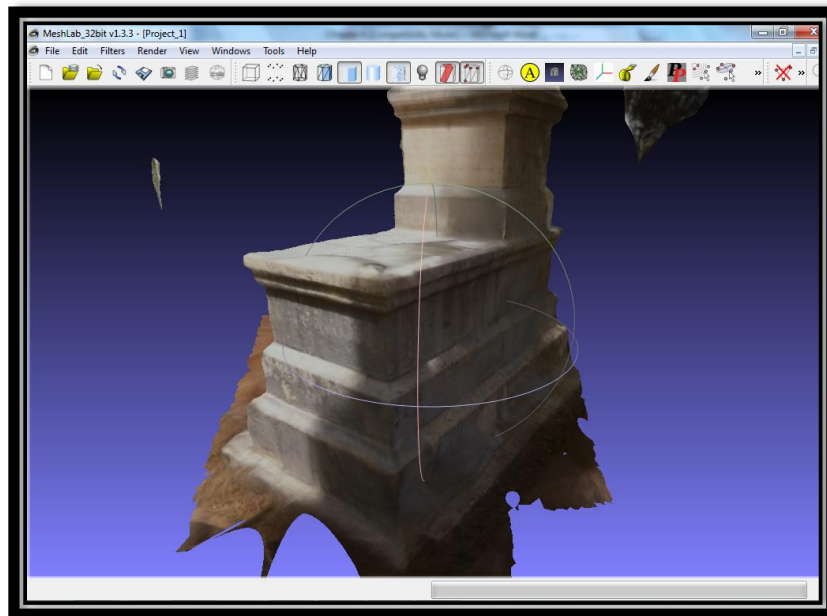


Figure (6 - 37) Cemetery as 3D model

CHAPTER SEVEN

CONCLUSIONS AND RECOMMENDATIONS

7.1 **Conclusions**

7.2 **Recommendations**

7.1 Conclusions

After the completion of this project, we conclude the following:

- Using many mobile phones (such as Nokia X3, iPhone 4G, iPhone 5s, Samsung Galaxy S4) were successfully used high accurate close range photogrammetry.
- The results of testing different models using different mobile phones are summarized in table (7-1). Here, we can easily find that the best results were obtained using I phone 5s camera. The worst results came from Nokia X3 mobile phone. But the Samsung Galaxy S4 caused problems when dealing with online services such as 123D Catch from Autodesk.

• Table (7 - 1) RMSE Results

phones	RMSE	Model 1	Model 2	Model 3	Model 4
Nokia X3		0.26998	0.300527	0.35075	0.31988
I phone 4G		0.11115	0.11769	0.111398	0.120526
I phone 5s		0.055289	0.046371	0.055632	0.034497

- These results could be achieved using freely available software (such as MeshLab, Agisoft Stereoscan, 123d catch, Insight 3d) to complete the tasks of testing procedure.
 - Insight3d: this program was rejected. There are several problems were occurring, when models were to be built.
 - Agisoft: this program was useful, because it is completely installed on the hard drive. It is working without the need of internet connection. A problem is that it deals with only a stereopair which causes limitations in many sided objects modeling.
 - Meshlab: this program was a useful tool for scaling rotating and measuring from the 3D models.
 - 123d Catch: it is an easy tool to create 3D models using large number of photos. Its only problem is that it is a tool on the cloud. It needs internet

connection. The user needs to upload large data size, when a high resolution camera is used.

7.2 Recommendations

After the completion of our project, the following points are recommended:

- Examination of more different mobile phones and professional/non-professional cameras.
- Examination of the effects and limitations of different object-camera distances.
- Examination different object sizes.
- Examination the use of close range photogrammetry by mobile phones and professional/non-professional cameras on the representation of topography.

References

Books

- [1] Paul R. Wolf and Bon A. Dewitt (2000), Elements of Photogrammetry (with application in GIS 3rd edition), The university of Wisconsin, Madison.
- [2] Dr. Ghadi Zakarneh (2007), Photogrammetry 2 Lecture notes, Palestine Polytechnic University, Hebron.

Scientific Papers

- [3] Clive Fraser, Harry Hanley and Simon Cronk , CLOSE-RANGE PHOTOGRAMMETRY FOR ACCIDENT RECONSTRUCTION , Department of Geomatics University of Melbourne , Victoria 3010 Australia (Dec. 1 2013).
- [4] Saiful Adilin Bin Ab Aziz, Zulkepli Bin Majid, Halim Bin Setan , APPLICATION OF CLOSE RANGE PHOTOGRAMMETRY IN CRIME SCENE INVESTIGATION (C.S.I.) MAPPING USING IWITNESS AND CRIME ZONE SOFTWARE , UTM-Photogrammetry and Laser Scanning Research Group , Infocomm Research Alliance (IcRA) Faculty of Geoinformation Science & Engineering Universiti Teknologi Malaysia ,(Dec. 1 2013).
- [5] 2003 Nova Award Nomination, Close-Range Photogrammetric Measurement for Structural Analysis , (Dec. 1 2013).
- [6] Murat YAKAR, Haci Murat YILMAZ and Omer MUTLUOGLU, Turkey, Data Collecting to Volume Computing Using Digital Close Range Photogrammetry and Laser Technics , (Dec. 1 2013).
- [7] Rami Al-Ruzouq and Shatha Kadhim , Close Range Photogrammetry and Neural Network for Facial Recognition , Department of Civil Engineering and Architecture , Faculty of Engineering, University of Bahrain, Manama Department of Computer Engineering , Faculty of Engineering, Al_Balqa' Applied University, Salt, Jordan , (Dec. 2 2013).
- [8] Sendo WANG , Yi-Hsing TSENG , AUTOMATIC SELF-CALIBRATION OF DIGITAL CAMERAS FOR CLOSE-RANGE PHOTOGRAMMETRY , National Cheng Kung University, China-Taipei , (Nov. 26 2013).

Websites

- [9] The World's Best Photos of camera and goerz - Flickr Hive Mind <http://flickrhivemind.net/Tags/camera,goerz/Interesting>, visited on (Dec. 1 2013).
- [10] PhotoInt - Hughha.co.uk , <http://www.hughha.co.uk/PhotoInt/PhotoInt.htm>, visited on (Dec. 1 2013).

- [11] The 6555th, Chapter III, Section 2, The Eastern Test Range in the 1950s
<http://www.fas.org/spp/military/program/6555th/6555c3-2.htm>, visited on
(Dec. 1 2013).
- [12] RELIEF (TERRAIN) DEPICTION - UNBC GIS
<http://www.gis.unbc.ca/courses/geog205/lectures/dem/index.php>, visited on
(Dec. 1 2013).
- [13] Product-geforce-3d-vision 2-wireless-glasses,
<http://www.nvidia.com/object/product-geforce-3d-vision2-wireless-glasses-us.html>, visited on (Dec. 1 2013).
- [14] X-ray, X-ray | Arabic encyclopedia of information , <http://ar-encyclopedia.blogspot.com/2010/11/x-ray.html>, visited on (Dec. 1 2013).
- [15] <http://insight3d.sourceforge.net/>, visited on (March. 15 2014).
- [16] <http://agisoft.ru/products/stereoscan>, visited on (March. 21 2014).
- [17] <http://www.123dapp.com/catch>, visited on (March. 25 2014).
- [18] <http://sourceforge.net/projects/meshlab/>, visited on (March. 4 2014).
- [19] <http://agisoft.ru/products/lens/>, visited on (April. 12 2014).

Maps

- [20] Hebron base map, Hebron municipality.